DOE/ET/37237--16
COO-2826-16
PNE-82-153

SCHOOL

OF

NUCLEAR ENGINEERING

Prepared for
The U. S. Department of Energy
Uner Contract No. DE-AC02-76ET37237

Purdue University

West Lafayette, Indiana 47907

DISCLAIMER

DOE/ET/37237--16
COO-2826-16
PNE-82-153

SCHOOL
OF
NUCLEAR ENGINEERING

DOE/ET/37237--16

DE82 021044

MASTER

FAST BREEDER BLANKET FACILITY
FBBF.
Annual Report
for the period January 1, 1981 -- December 31, 1981

Edited by

F. M. Clikeman

Prepared for

The U. S. Department of Energy
Under Contract No. DE-AC02-76ET37237

July, 1982

Purdue University, West Lafayette, Indiana 47907

Purdue University
West Lafayette, IN 47907

SCHOOL OF NUCLEAR ENGINEERING

FAST BREEDER BLANKET FACILITY

Principal Investigators

K. O. Ott
F. M. Clikeman

ANNUAL REPORT for 1981

Edited by F. M. Clikeman

Results reported in this report include preliminary data and are subject to revision.

Work prepared for the auspices of the

U. S. DEPARTMENT OF ENERGY

NOTICE

Abstract

This annual report contains a summary of fission rate, spectra, and gamma-ray heating rate measurements made in the first blanket of the Purdue Fast Breeder Blanket Facility. The first blanket consisted of aluminum clad, natural UO_2 fuel rods with a secondary cladding of stainless steel or aluminum. The blanket was arranged in two concentric regions around the neutron source and converter regions. A neutron diffusion code, 2DB, and a Monte Carlo code, VIM, both using homogeneous cross section groups have been used to calculate the reaction rates. Calculated to experimental values for a number of important reactions are presented. A modified method of applying Bondarenko self-shielding factors to correct for the self shielding of resonance energy neutrons in aluminum, stainless steel and UO_2 has improved the agreement between the calculations and experiment, but does not account for all of the differences. Work is continuing on improvement of the calculations, both in the area of sensitivity studies of various cross sections and in the area of improvement in the corrections for the heterogeneity effect. Experimental work on blanket II, a two sector (each 180^{o}) blanket is progressing

CONTENTS

LIST OF FIGURES

I. INTRODUCTION

This report covers the progress made on the Purdue Fast Breeder Blanket Project during a period of time from January 1, 1981 through December 31, 1981. During this period of time the major emphasis of the project has been to complete the experimental measurements on blanket I, analyze the results, and start measurements on blankets IIA and IIB. Blanket I, 0.510 m thick, consisted of two regions. The inner region consisted of natural uranium oxide fuel rods, aluminum clad, with a secondary cladding of stainless steel. The outer region, 0.170 m thick, consisted of the same type of aluminum clad natural uranium oxide fuel, but with a secondary cladding of aluminum. The fuel rods were equally spaced in a uniform hexagonal pattern and were supported by grid plates at the top and bottom of the blanket region, minimizing the amount of structural material in the blanket. All measurements have been complete in blanket I. Final analyses of the fission rate measurements and neutron spectra measurements have been completed and have been reported as Ph.D. theses[1,2]. Project reports based on these measurements are now being prepared. Neutron capture rate measurements and thermoluminescent dosimeter measurements of the gamma-ray heating are still being analyzed and will be reported in the 1982 annual report and in project reports.

Analysis of the measurements show that the reaction rate calculations using two-dimensional diffusion theory codes are in error by as much as 35% in the outer regions of the blankets. A new cross section set, calculated for the as built facility, failed to improve the agreement between the experimental and calculated results. A modified method of applying the Bondarenko corrections for neutron resonances has been

tried and has reduced the disagreement between the calculated and experimental neutron capture rates in ^{238}U and ^{197}Au.

Blanket II uses the same grid plates as blanket I, but rather than having two concentric regions, the blanket has to 180^{o} sectors. The natural uranium fuel rods in blanket IIA have a secondary cladding of stainless steel while the rods in IIB have a secondary cladding of aluminum. Thus, blanket IIB has no stainless steel, but increased amounts of aluminum. Blanket II will provide opportunities for the direct comparison of measurements in blankets will diffenent amounts of aluminum and stainless steel. Neutron reaction rate measurements, spectrum measurements and gamma ray heating rate measurements are now being carried out in blankets II.

II. EXPERIMENTAL MEASUREMENTS IN THE FBBF

II.A Fission Rate Measurements in the FBBF

(H. Chou, R Johnson, and F. Clikeman)

Fission rates have been measured using the fission tract recorder technique. Five thin fission foils (< 1 mg/cm^2) containing the nuclides ^{232}Th, ^{235}U, ^{237}Np, ^{238}U, and ^{239}Pu were used as well as thick (> 40 mg/cm^2) depleted uranium and thorium foils. Fused quartz was used as the recorder medium. Fission rates are measured by placing a fission foil and a recorder inside a holder. The holder is then positioned between fuel pellets in an experimental fuel pin. After irradiation, the number of fissions recorded by the recorder is obtained using an automatic track counting system[3]. Radial fission rate distributions have been made in blanket I at the active midplane located approximately 0.47 m from the bottom of the fuel pins. Reproducibility of the measurements is ±3%.

Calculations of the measured fission rates have been carried out using both the two-dimensional diffusion code 2DB[4] and the continuous energy Monte Carlo code VIM[5]. The 30-group cross section set used in the 2DB calculation were generated using a homogeneous Bondarenko[6] self-shielding factor. A more detailed discussion of the experimental methods and calculations can be found in Reference 7.

As shown in Figs. 1 and 2, the diffusion calculation greatly under-predicts the ^{235}U and the ^{239}Pu fission rates at large radii. The 2DB C/E values range from 1.08 to 0.74 for ^{235}U and from 1.03 to 0.71

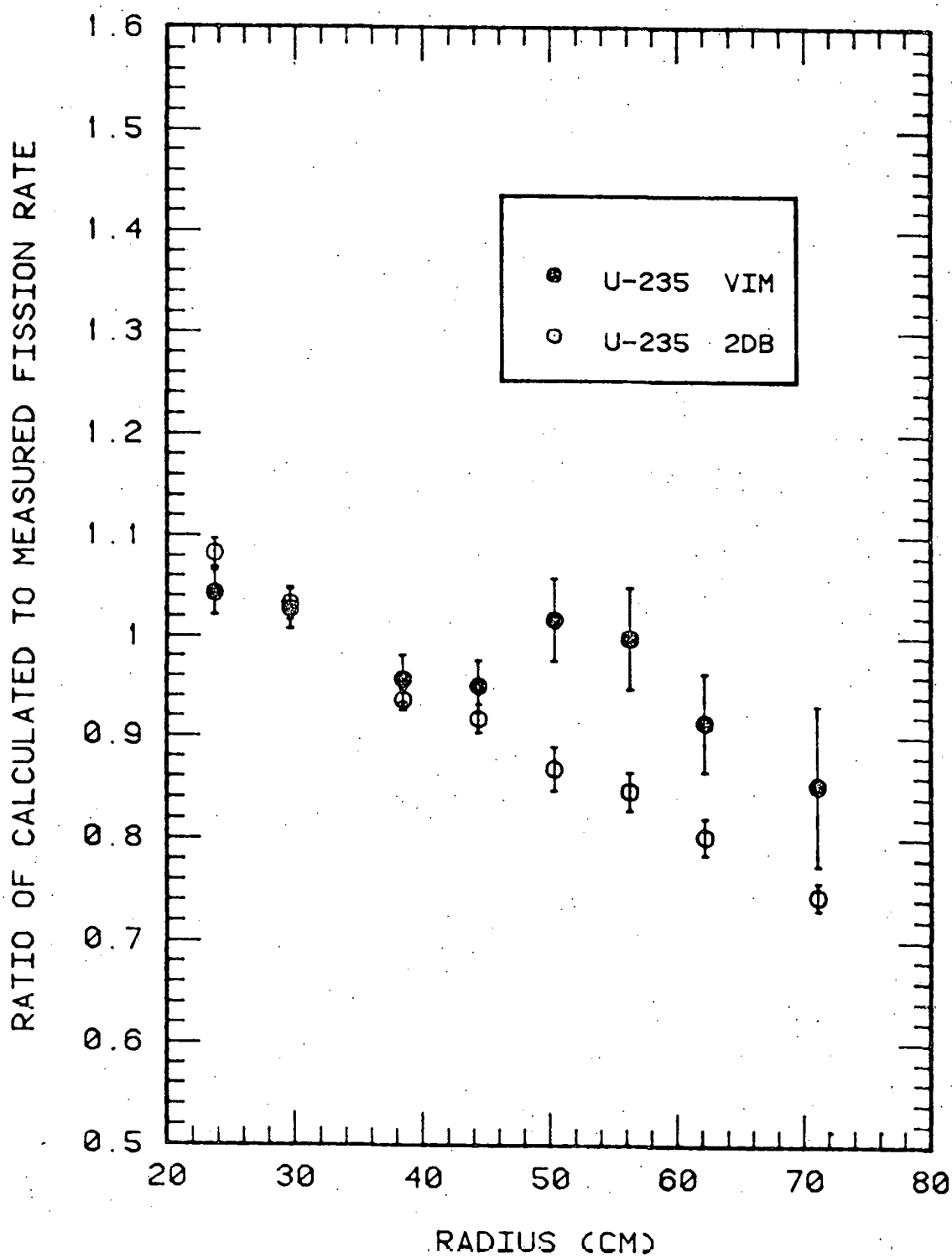

Figure 1: Ratio of calculated to measured fission rates of ^{235}U.

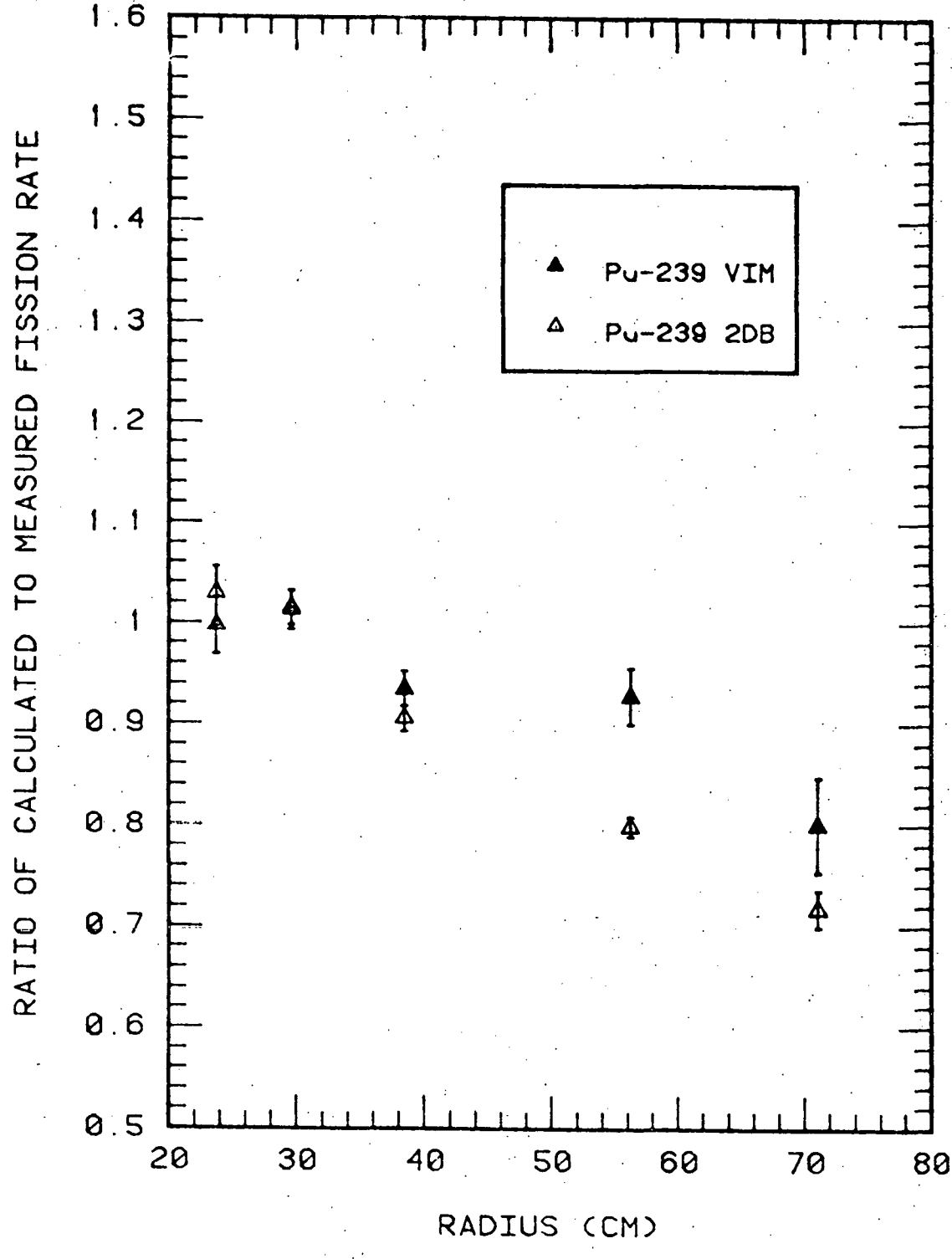

Figure 2: Ratio of calculated to measured fission rates of ^{239}Pu.

for ^{239}PU. The 2DB C/E values decrease steadily with increasing radius at the same rate for both nuclides. In contrast, the Monte Carlo transport calculation gives better agreement, although the Monte Carlo calculation also underpredicts the ^{235}U and ^{239}Pu fission rates at large radii. The VIM C/E values range from 1.04 to 0.85 for ^{235}U and from 1.0 to 0.8 for ^{239}Pu.

The spectral indices based on the ^{235}U fission rate were also determined. Spectral indices are commonly reported in fast reactor core and blanket measurements because systematic error sources such as power level and counting efficiencies cancel out. In the present measurements, the systematic errors of the spectral indices are dominated by the statistical errors of the foil masses; systematic errors due to the neutron source strength, efficiency, and foil holder perturbatiions cancel. For FBBF fission ratios obtained using thin foils only, the systematic error is estimated to be within 1%, except for the ^{232}Th which is estimated to be 3%. For fission ratios using thick foils, the systematic errors are estimated to be 2% for ^{232}U and 4% for ^{232}Th. Figure 3 shows the ratios of calculated to measured spectral indices based on the ^{235}U fission rate. The errors plotted are statistical errors only. Both the diffusion and the Monte Carlo calculation predict the ^{239}Pu to ^{235}U fission ratios very well throughout the blanket region.

Neither the diffusion nor the Monte Carlo calculation, however, correctly predicts threshold fission rates. The diffusion calculation underpredicts the ^{237}Np to ^{235}U and the ^{232}Th to ^{235}U fission ratios but overpredicts the ^{238}U to ^{235}U fission ratio. The Monte Carlo calculation gives similar results at small radii but the C/E values increase

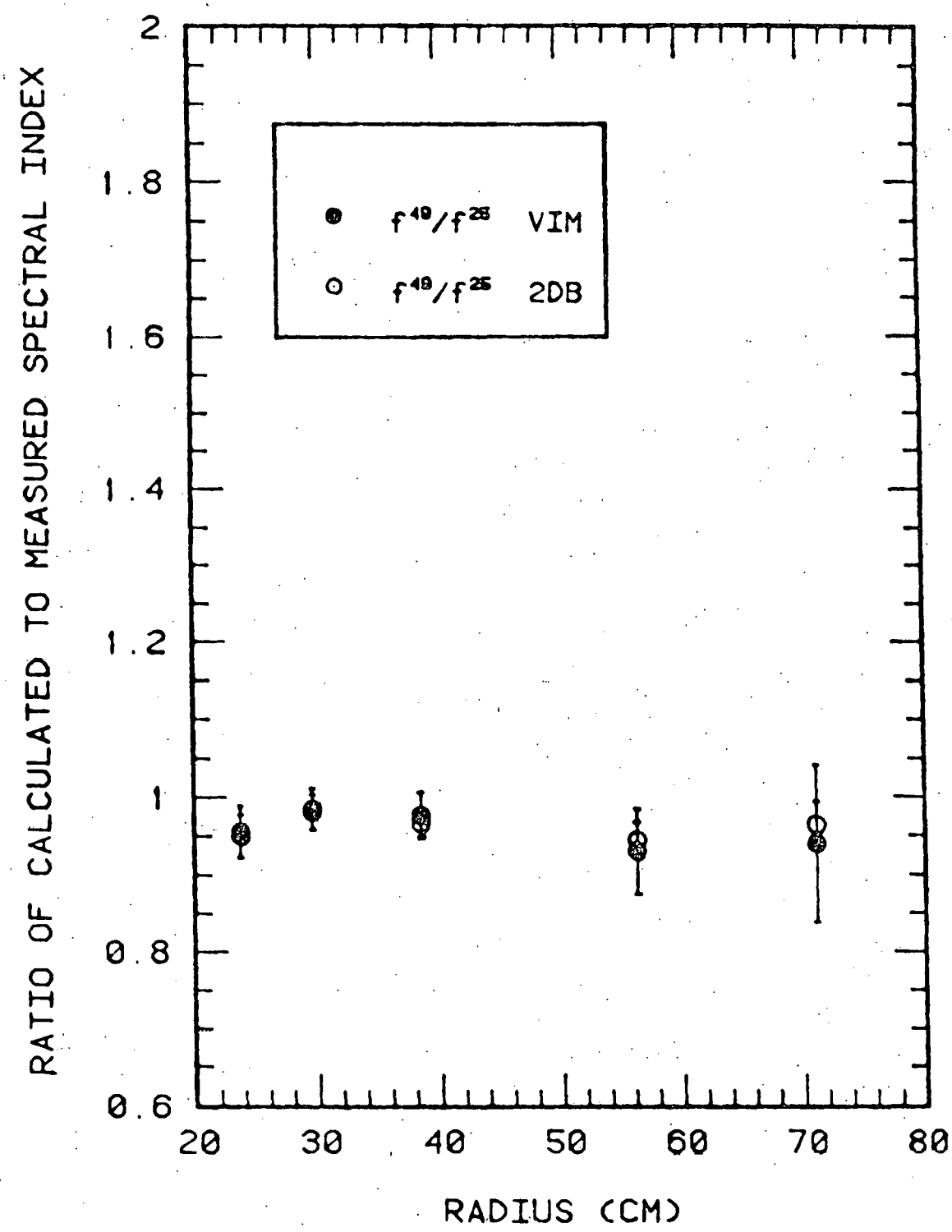

Figure 3: Ratio of calculated to measured ^{239}Pu to ^{235}U fission ratio.

with increasing radius.

Figure 4 gives the C/E results of ^{237}Np which has a low and poorly defined threshold of approximately 0.6 MeV. The diffusion calculation again greatly underpredicts the ^{237}Np fission rates at large radii; the 2DB C/E values drop from 0.91 to 0.60 with a slope similar to the 2DB C/E curves of ^{235}U and ^{239}Pu. The Monte Carlo calculation underpredicts the ^{237}Np fission rates by 10% throughout the blanket region.

As shown in Fig. 5, the diffusion calculation greatly overpredicts the ^{238}U fission rates at small radii. Agreement between the diffusion calculation and the measurements is good at large radii; this agreement, however, is probably coincidental. The Monte Carlo calculation overpredicts the ^{238}U fission rates by 20 to 40%.

Figure 6 shows the C/E results of ^{232}Th which has a fission threshold at approximately 1.2 MeV. The diffusion calculation underpredicts the ^{232}Th fission rates at large radii. The 2DB C/E values range from 1.0 to 0.75; the values decrease with a steeper slope in the inner blanket and tend to tail off in the outer blanket. The Monte Carlo calculation, however, overpredicts the fission rates at large radii. The VIM C/E values ranges from 0.96 to 1.15 with a maximum value at the inner-outer blanket interface.

The various comparisons indicate that present diffusion calculations are inadequate for predicting ^{235}U, ^{238}U, and ^{239}Pu fission rates in thick radial uranium blankets of fast breeder reactors. Furthermore, power production within such a blanket would also be inadequately predicted by diffusion calculations. Monte Carlo transport calculations

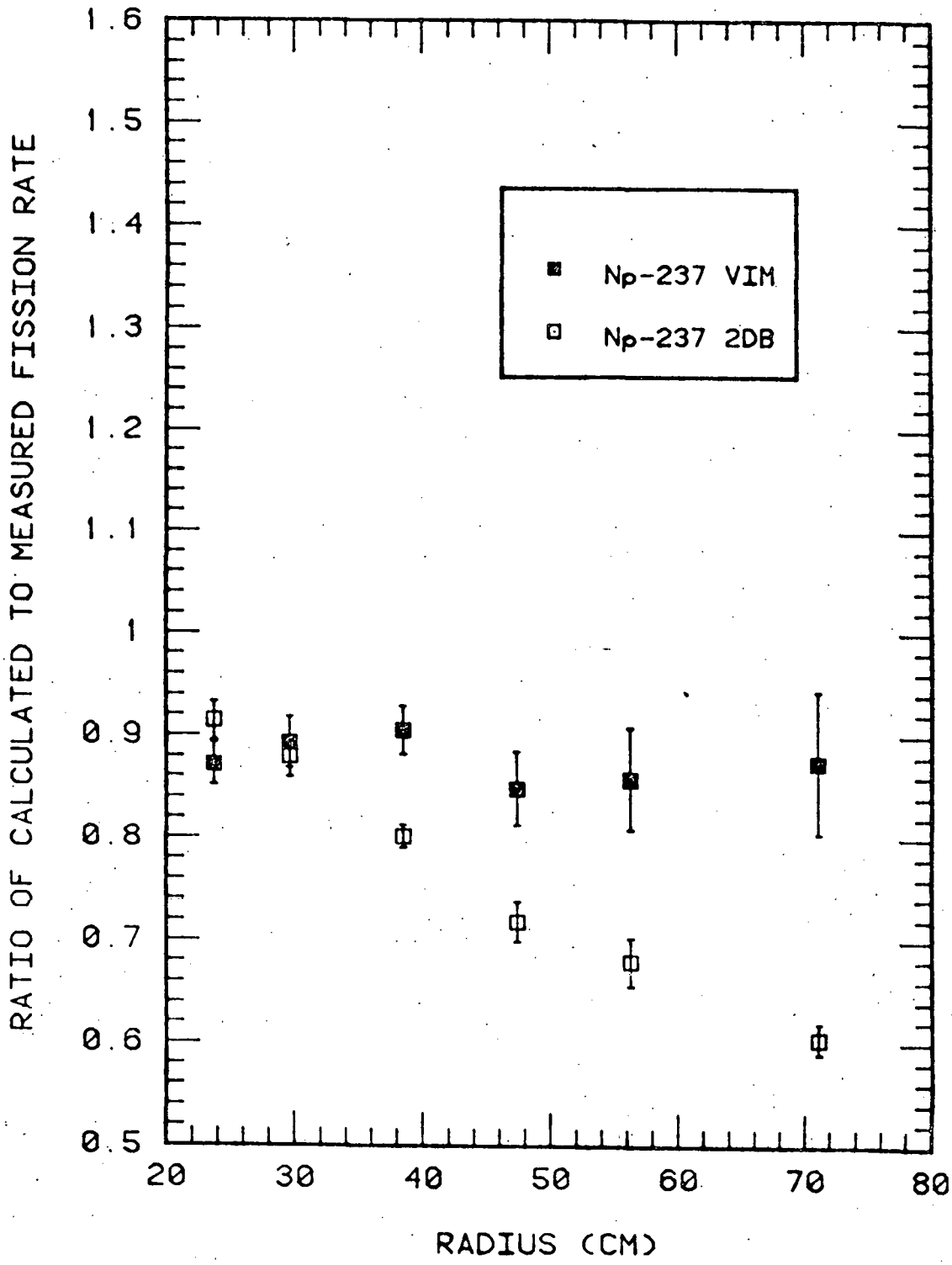

Figure 4: Ratio of calculated to measured fission rates of ^{237}Np.

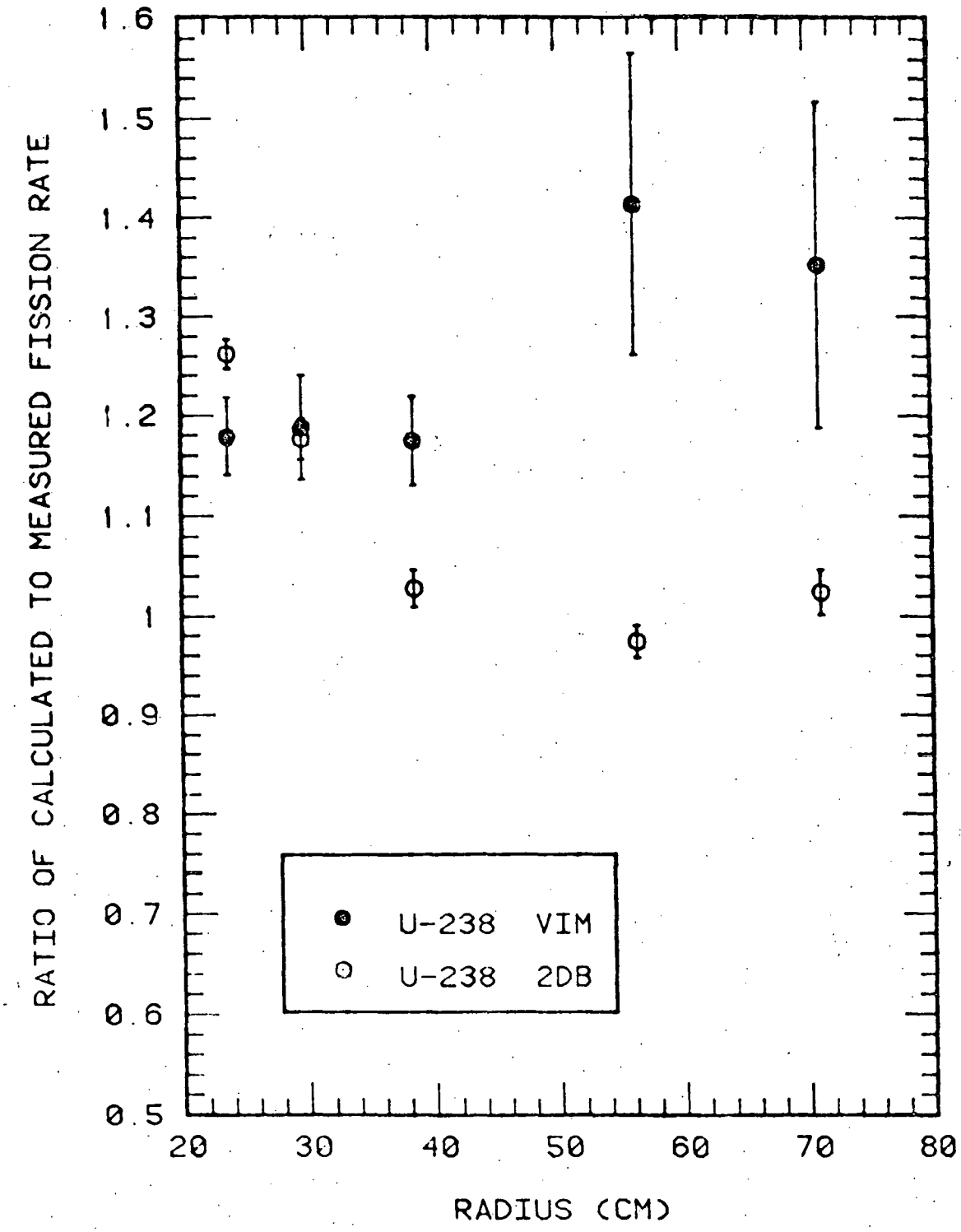

Figure 5: Ratio of calculated to measured fission rates of ^{238}U.

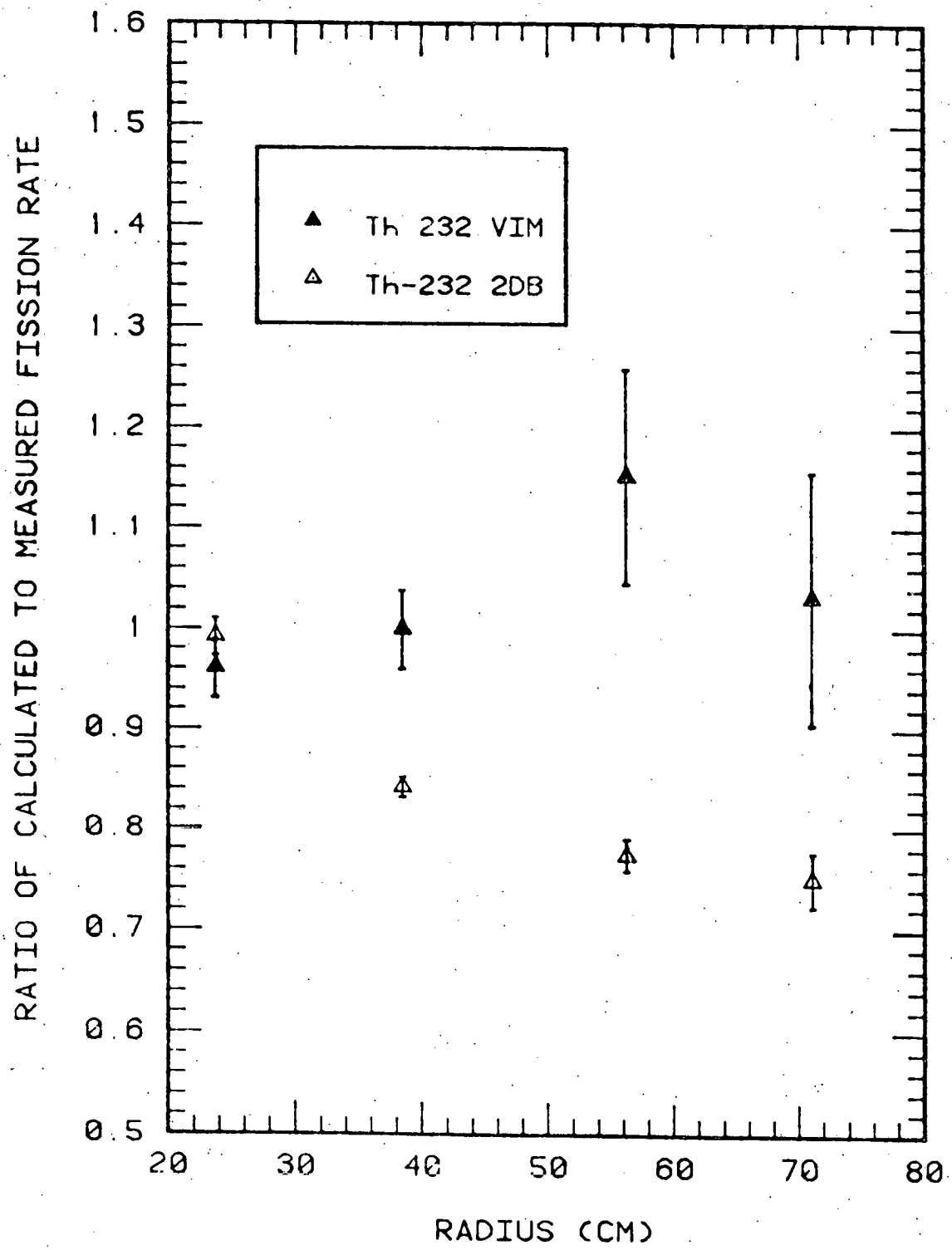

Figure 6: Ratio of calculated to measured fission rates of ^{232}Th.

give better predictions in blanket regions than diffusion calculations. The overprediction of ^{238}U fission rates by the Monte Carlo transort calculation is attributed to difficiencies in ENDF/B-IV data for one or more nuclides above 1 MeV; the current results do not suggest which nuclide is the major cause of the overprediction, however. The comparison of spectral indices indicates that the ^{235}U and ^{239}Pu fission cross sections used in the 2DB and the VIM calculations are consistent.

In summary, the diffusion calculation greatly underpredicts the ^{232}Th, ^{235}U, ^{237}Np, and ^{239}Pu fission rates at large radii and overpredicts the ^{238}U fission rates at small radii. The Monte Carlo transport calculation predicts the ^{232}Th, ^{235}U, ^{237}Np, and ^{239}Pu fission rates reasonably well but greatly overpredicts the ^{238}U fission rate throughout the blanket region. For ^{235}U and ^{239}Pu, the VIM and 2DB fission rates are within 5% in the first 20 cm into the blanket. The differences increase to 15% at the blanket's outer boundary. For ^{232}Th, ^{237}Np, and ^{238}U (all of which exhibit threshold fission) the VIM and 2DB fission rates agree reasonably well in the first 10 cm into the blanket, but large differences are observed in the outer blanket.

II.B Neutron Spretra Measurements

(D. Vehar and F. Clikeman)

Neutron energy spectra have been experimentally determined for a number of blanket locations. Measurements were made at radial positions 0.385, 0.563 and 0.711 m from the center of the facility. Spectra were determined for five axial positions at each radial position. The axial positions measured, from the bottom of the fuel in the transformer region to the center of the sensitive region of the detector, were 0.025, 0.243, 0.460, 0.678 and 0.895 m. These five heights are equally spaced, with 0.46 m corresponding to the midplane of the active fuel in the FBBF transformer region. A height of 0.025 m represents the lowest height to which a proton-recoil detector can be inserted, while a height of 0.895 m is about 0.33 m below the top of the fuel in the blanket. Although other types of measurements have been made at locations with radii less than 0.385 m, the neutron flux is great enough at these radii to cause detector saturation and excessive dead times with the proton-recoil counters. Measurements could therefore not be made at radii less than 0.385 m.

Figures 7 through 11 show neutron energy spectra for representative locations. The data are presented on an absolute basis for a neutron source strength of 10^{10} neutrons per second. The solid lines represent spectra determined by a two-dimensional diffusion calculation using the code 2DB[4]. The experimental data are presented in the figures as vertical bars representing $\pm$ one standard deviation statistical error, based only on counting statistics. Systematic errors are not shown, but are

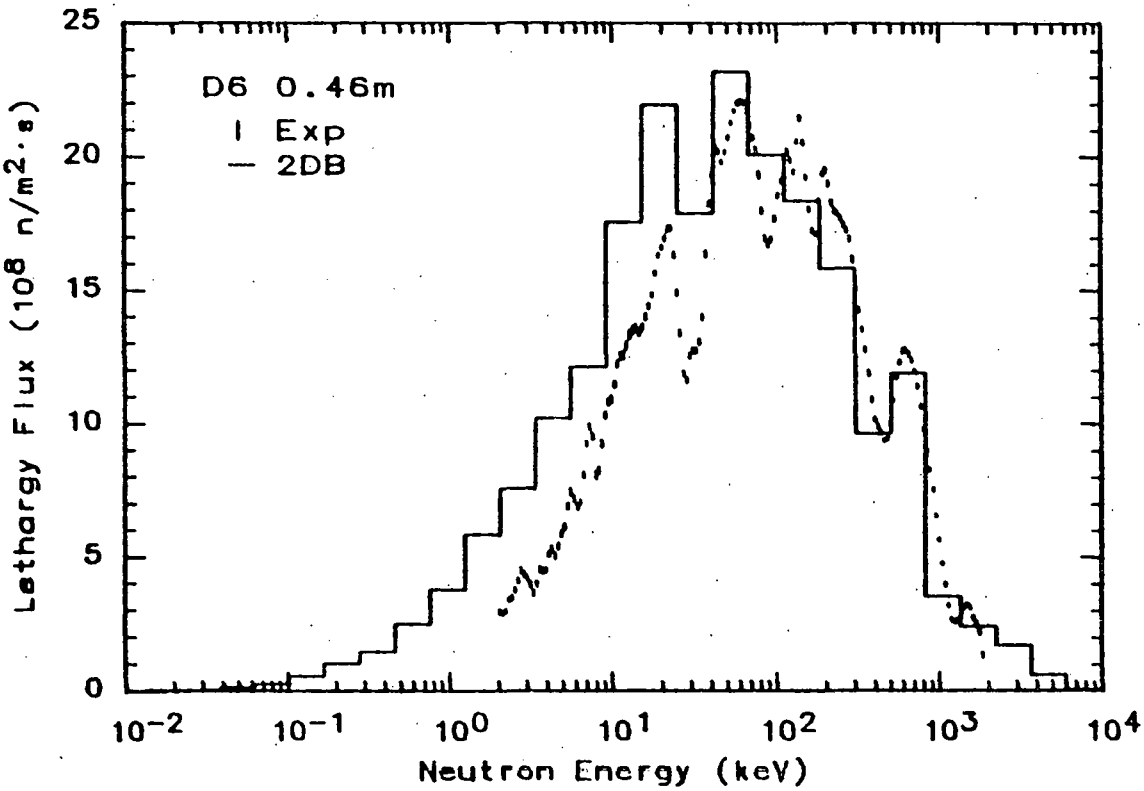

Figure 7: Neutron energy spectra for radius of 0.385 m and height of 0.460 m. The vertical bars represent statistical errors (one standard deviation). The solid line is the two-dimensional diffusion calculation.

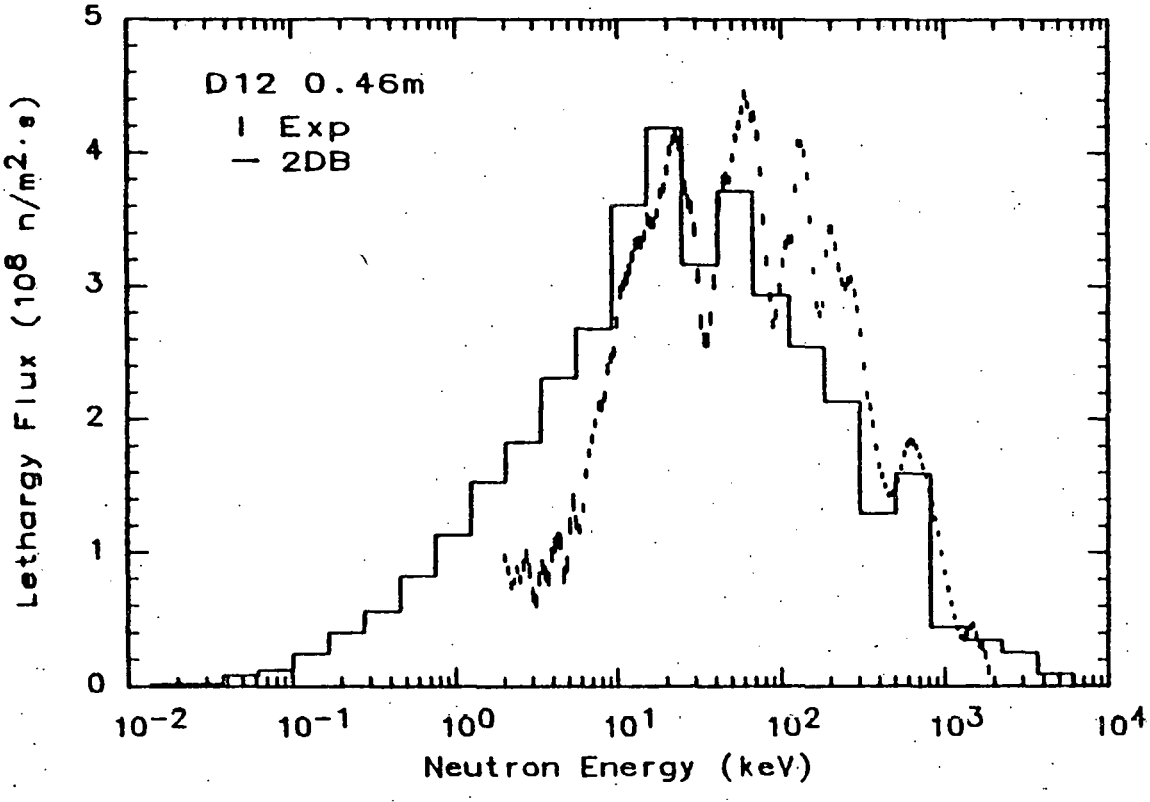

Figure 8: Neutron energy spectra for radius of 0.563 m and height of 0.460 m. The vertical bars represent statistical errors (one standard deviation). The solid line is the two-dimensional diffusion calculation.

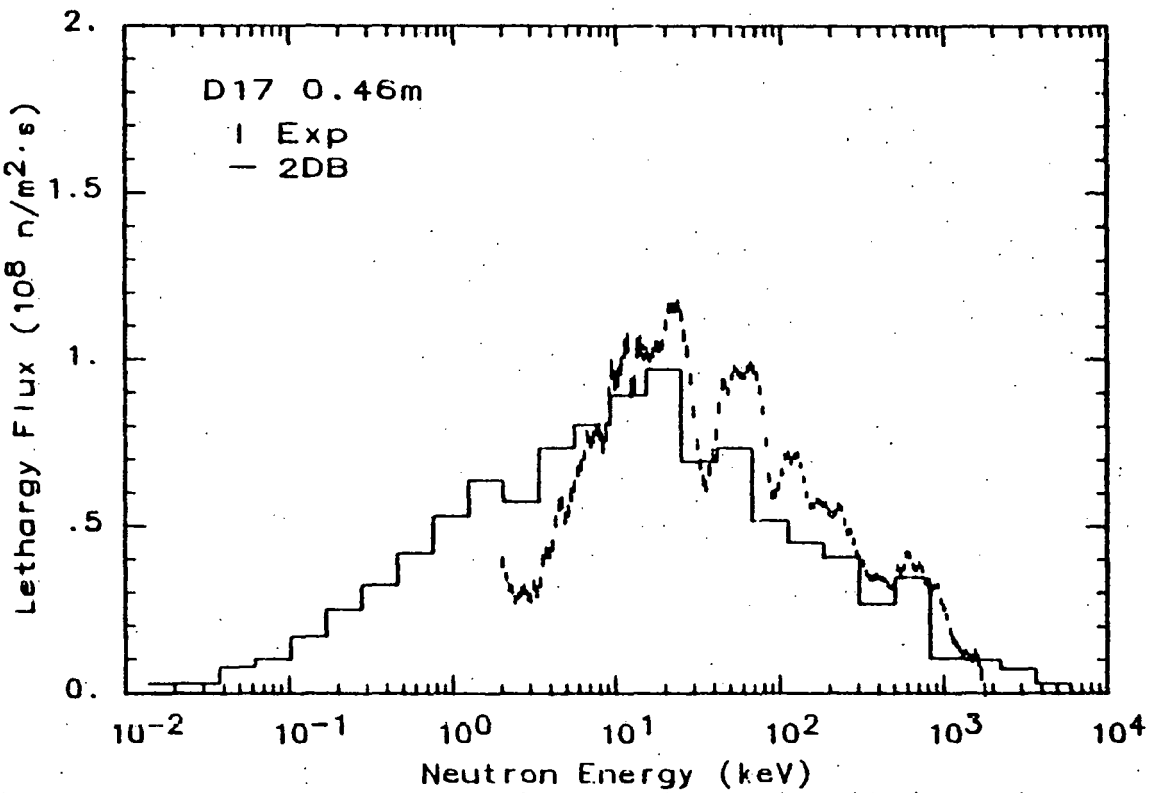

Figure 9: Neutron energy spectra for radius of 0.711 m and height of 0.460 m. The vertical bars represent statistical errors (one standard deviation). The solid line is the two-dimensional diffusion calculation.

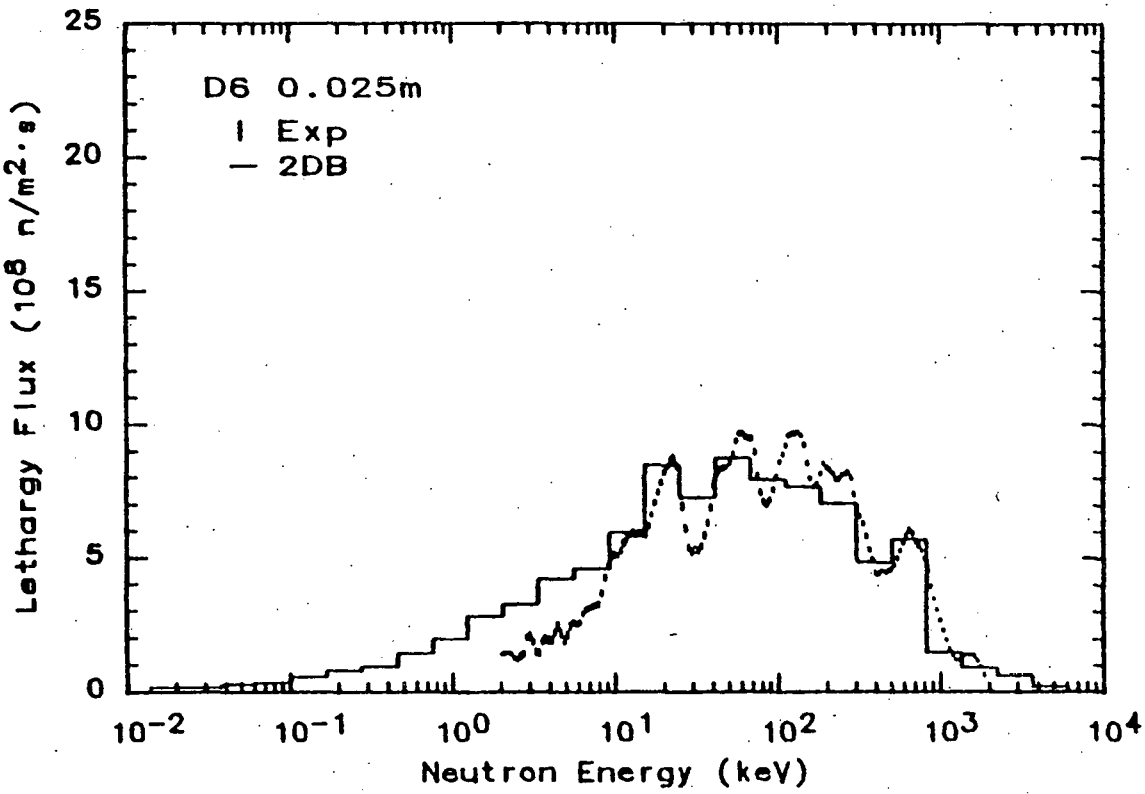

Figure 10: Neutron energy spectra for radius of 0.385 m and height of 0.025 m. The vertical bars represent statistical errors (one standard deviation). The solid line is the two-dimensional diffusion calculation.

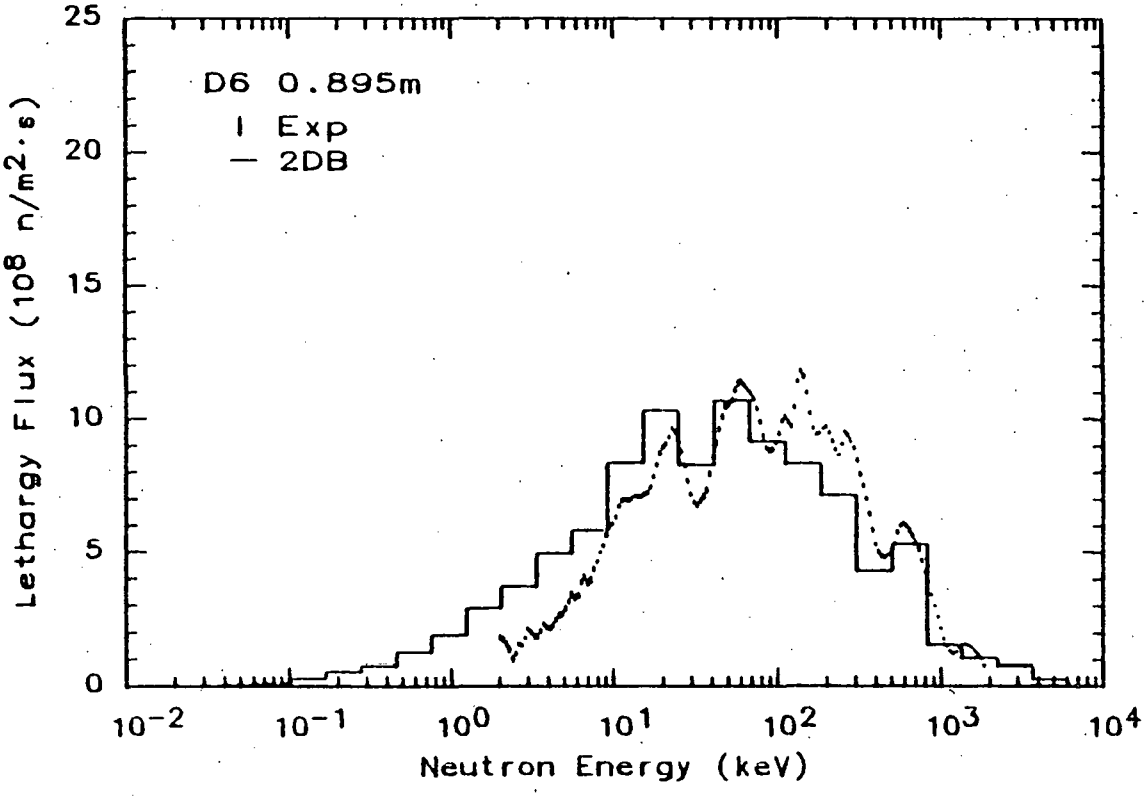

Figure 11: Neutron energy spectra for radius of 0.385 m and height of 0.895 m. The vertical bars represent statistical errors (one standard deviation). The solid line is the two-dimensional diffusion calculation.

estimated to be about 8 percent in the energy region above 10 keV and as much as 22 percent in the region below keV. Sources of systematic error considered include source strength, detector sensitivity, energy calibration, energy/ion pair, and corrections to proton recoil data. The total systematic errors are obtained by summing the individual errors. It is recognized that when there are a large number of independent systematic errors of comparable magnitude, summing in quadrature may be more appropriate. The total errors may, therefore, be overly conservative. Much of the uncertainty in the spectra below 10 keV is attributed to uncertainty in W, the energy required to produce an ion pair. As expected, the experimental spectra show finer detail than do the calculated spectra, due to the relatively large group widths used for the calculation.

Several trends are apparent from the figures. First, the exprimentally determined spectra are harder than the calculated spectra. That is, the calculated neutron spectra have higher average lethargies (lower average energies). This is illustrated in Table 1 where average lethargies for calculated and experimental spectra are presented as a function of detector location. Average lethargies were determined over the energy range between 1.234 keV and 1353 keV, weighted with the group flux per unit lethargy. This energy range corresponds to the calculational energy groups 5 through 18, the groups covered completely by the proton-recoil measurements, and represents between 80 and 93% of the calculated neutron flux at the midplane. The best agreement between the calculated and experimental spectra is achieved at a height of 0.025 m, with the detector near the steel base plate at the bottom of the

Table 1 Average Lethargy as a Function of Detector Location.

Location		Average Lethargy Groups 5 - 18[a]		
Radius	Height	Calculated	Experimental	C/E
meters				
0.385	0.025	3.235	3.388	1.047
0.385	0.243	3.222	3.422	1.062
0.385	0.460	3.240	3.425	1.057
0.385	0.678	3.224	3.424	1.062
0.385	0.895	3.257	3.449	1.059
0.563	0.025	3.394	3.524	1.038
0.563	0.243	3.422	3.591	1.049
0.563	0.460	3.377	3.592	1.063
0.563	0.678	3.423	3.592	1.049
0.563	0.895	3.348	3.605	1.043
0.711	0.025	3.584	3.635	1.014
0.711	0.460	3.594	3.759	1.046
0.711	0.895	3.609	3.761	1.042

[a] $u(E) = \ln(10/E)$, E in MeV.

blanket. There, the neutron spectrum is dominated by neutrons scattered back into the blanket by the steel base plate, due to the large iron scattering cross section. At other locations, the detector is well within the fueled region of the blanket and does not see the effects of the iron.

The second effect seen in the figures is that the magnitude of the calculated spectra tends to decrease more rapidly with radius than the magnitude of the experimental spectra. The experiment is overpredicted at location 0.385 m and underpredicted at location 0.711 m. Again, the agreement between the calculation and the experiment is best at a height of 0.025 m, near the steel base plate.

Based on the spectrum measurements alone, little can be said regarding the reasons for the discrepancies between the calculated and experimental neutron energy spectra, since any of several reactions could be at fault. Underestimating the number of fissions, either by undercalculation of the number of neutrons or inaccurate fission cross sections for ^{235}U and ^{238}U, directly affects both the magnitude of the flux and the spectral hardness, since fission neutrons are relatively high in energy. The result is a calculated spectrum that is softer and which drops off too rapidly with blanket radius. This conclusion is consistant with the results of the fission rate measurements reported in the preceeding section. Other mechanisms which could also account for a decrease in the calculated high energy spectra are overestimating the amount of leakage which, will also result in a decreased magnitude, and assuming that faster neutrons have a larger mean free path, will cause the calculated spectrum to become softer. Overestimating the amount of

scattering, particularly inelastic scattering, reduces both the spectral hardness and the magnitude of the flux.

A secondary effect from either overestimated scattering or overestimated leakage is a further reduction of magnitude and spectral hardness indirectly through reduced fission. That is, a softer spectrum results in fewer fast fissions in ^{238}U, while a reduced magnitude results in fewer fissions in both ^{238}U and ^{235}U. However, the number of fissions from ^{238}U is small compared to that from ^{235}U (calculated to be 4.4×10^{-3} at the r = 0.385 m midplane and 1.8×10^{-3} at the r = 0.711 m midplane), so that the effect from ^{238}U fission is probably negligible.

Overestimation of neutron absorption also reduces the magnitude of the calculated flux. However, since lower-energy neutrons are more readily absorbed (lower-energy neutrons may see resonances which do not affect the higher-energy neutrons), overestimating the amount of absorption tends to harden the calculated spectrum, contrary to what is observed. Measured neutron capture rates in ^{238}U, discussed in Sec. IID, show that the calculations underpredict the reaction, also confirming that this is probably not the source of the problem. Two reports, covering the details of the experimental methods and the results of the spectrum measurements in blanket I are being prepared.

Sprectrum measurements are now being made in blanket II, with special emphasis being given to the high energy portion of the spectrum where fission rate measurements with the threshold reactions have indicated considerable disagreement the calculations (see Sec. IIA).

II.C Gamma-Ray Heating Measurements

(Ken Koch and F. Clikeman)

The determination of gamma-ray heating rate distributions in Liquid Metal Fast Breeder Reactors, LMFBRs, is of importance for the optimization of cooling requirements in the various reactor regions. Approximately 7% of the total fission energy is released in the form of gamma rays and an almost equivalent energy release is in the form of gamma rays from neutron capture.

Gamma-ray dosimetry measurements can be made using a wide variety of gamma-ray sensitive devices. Thermoluminescent dosimeters, TLDs, have been used quite successfully for gamma-ray heating measurements in zero-power fast reactors. Small size, low neutron sensitivity, and simplicity of use are major advantages for using TLDs for gamma-ray heating measurements instead of other devices.

The interpretation of TLD measurements in a reactor environment presents unique problems in relating the TLD dose to the dose in the surrounding material and in determining neutron responses of the TLDs. Corrections for the relation of the TLD dose to the dose in the surrounding material have been developed from cavity ionization theory and have become known as f-factors. These corrections are sometimes called gamma-ray spectral effect corrections since they are dependent on the gamma-ray spectrum during irradiation. The corrections are required because of the "mismatch" of properties of the TLD and the surrounding material; this leads to different doses in the TLD and in the surrounding material. Corrections for neutron sensitivity are not as well

developed due to the limited neutron sensitivity data available for the types of TLDs used in these experiments. However, the use of TLDs with extremely low neutron sensitivities such as ^{7}LiF and CaF_2 has minimized these neutron corrections.

In almost all of the recent programs of gamma-ray heating measurements, the TLD results have been compared to calculated gamma-ray heating rates. These comparisons have indicated that the calculational methods used in determining gamma-ray heating rates provide accurate results only in the core regions of LMFBRs. The inaccuracies of the calculations increase with increasing distance from the core. These results contribute to the motivations for making TLD gamma-ray heating measurements in a benchmark fast breeder reactor blanket facility.

Gamma-ray heating measurements were made in the Fast Breeder Blanket Facility, FBBF, using stainless steel and lead sleeves. Stainless steel heating measurements are of primary interest because of the extensive use of stainless steel in the cladding and structural components of a fast reactor. Lead was chosen for gamma-ray heating measurements because its atomic number and density are similar to that of uranium dioxide. It was desirable to obtain heating data that would be comparable to gamma-ray heating in uranium dioxide since the majority of gamma-ray energy deposition is in the fuel. Lead heating measurements are also of importance for studying the application of reported analysis methods for TLD gamma-ray heating measurements in high atomic number materials, specifically relating to f-factors.

The use of lead as one of the mediums for gamma-ray heating meas-

urements was one of the primary reasons for choosing CaF_2 TLDs over LiF TLDs. The CaF_2 TLDs have a higher effective atomic number than LiF, which helps to minimize material "mismatches" between the TLDs and the lead sleeves. This is desirable in order to keep the f-factors closer to unity thereby minimizing the uncertainties in this correction.

Irradiations were made in the FBBF for radial traverses through the blanket at a height of 0.45m to 0.46m from the bottom of the blanket; this height corresponds to the axial midplane of the converter's active fuel. Irradiations were also made for axial traverses with stainless steel sleeves at experimental positions corresponding to radii of 0.2369m, 0.3849m, 0.5626m, and 0.7106m. All FBBF irradiations were made using sleeves with four TLDs. Each sleeve irradiation then yielded four TLD responses which were averaged to give an average response for that sleeve position.

The objective of the FBBF gamma-ray heating measurements was to obtain heating rates due to gamma rays found in LMFBR blankets during steady state operation. These gamma-rays come from various sources: fission reactions, capture reactions, fission product and activation product decay, and the natural activity of the uranium fuel. Most reactor analysis calculations do not include the natural activity of the fuel as a gamma-ray source; this is because it is negligible in actual power reactors. However, since the FBBF has much lower flux densities, the natural activity of the fuel is no longer negligible, especially near the outer edge of the blanket where the gamma-ray fluxes are very small. Thus, to compare the FBBF gamma-ray heating measurements to calculated gamma-ray heating rates, the natural activity of the fuel must

be considered. This was done by taking measurements with the neutron source both in position and removed from the facility. The measurements with the source removed can be subtracted from the measurements made with the source in position to eliminate the gamma-ray dose contributions due to the natural activity of the fuel.

All net dose rates were normalized to a reference FBBF neutron source strength of 1×10^{10} neutrons per second. The normalization of all gamma-ray heating rates to a reference source strength of 1×10^{10} neutrons per second allows all the measured gamma-ray heating rates to be compared to a calculation based on the same source strength.

The term, f-factor, applies to corrections applied to TLD/sleeve combinations to relate the TLD dose to the sleeve dose. A f-factor is defined as the ratio of the dose received by the TLD to the dose received by the surrounding sleeve material. They are based on cavity ionization theory and can be used to determine the gamma-ray heating in the sleeve material from a measured TLD dose. The dose received by the sleeve material can be found as

$$D_z = 1/f \cdot D_{TLD}$$

where:

D_{TLD} = dose recieved by the TLD,

D_z = dose received by the sleeve material, and

f = f-factor for the particular TLD/sleeve combination irradiated in a particular gamma-ray spectrum.

The neutron fluxes required for the TLD analysis were calculated using the two-dimensional neutron diffusion code 2DB[4]. The neutron fluxes were calculated in 30 energy groups using a source calculation with the explicit modeling of the 4 ^{252}Cf neutron sources used to drive the FBBF. These 30 group cross sections were collapsed from the 50 group LIB-IV[8] cross section library using the one-dimensional diffusion code 1DX[9]. The 1DX code and the LIB-IV cross section library use the Bonderanko[6] self-shielding factor method for resonance self-shielding. All isotopes in the FBBF calculation were self-shielded using this method based on the region in which each isotope is located. The one-dimensional model of the FBBF used in 1DX was a radial slice through the FBBF at the transformer active fuel midplane.

The gamma-ray fluxes and heating rates in stainless steel and lead required for the TLD analysis were calculated using the one-dimensional transport code, ANISN[10]. The gamma-ray cross sections, the gamma-ray production cross sections, and the gamma-ray kerma factors used in these calculations were from the coupled neutron/gamma-ray DLC-37/EPR[11] cross section library. From the gamma-ray flux calculations, it was found that the ^{238}U capture reaction dominated the gamma-ray production.

The gamma-ray cross sections of the coupled neutron/gamma-ray cross section set were extracted and used in ANISN to calculate the gamma-ray fluxes for a radial geometry model representing a slice through the FBBF at the transformer active fuel midplane. A distributed gamma-ray source was calculated from the calculated neutron fluxes and the gamma-ray production cross sections of the DLC-37/EPR library. This distributed source was used as an external source for the ANISN gamma-ray flux

calculation. It is important to realize which gamma-ray sources are included in such a calculation. The DLC-37/EPR gamma-ray production cross sections only include gamma rays produced in fission reactions and prompt gamma rays produced in capture reactions. The decay gamma rays of activation products and the natural decay of the uranium fuel are not included.

Gamma-ray heating rates in stainless steel and lead were determined from the calculated gamma-ray fluxes and the kerma factors of the DLC-37/EPR library. The heating rates in lead were calculated directly from the lead kerma factors, while the stainless steel heating rates had to be determined by adding the heating rates of the constituents together.

The measured gamma-ray heating rates in stainless steel for radial traverses of the FBBF are shown in Figure 12. The gamma-ray heating rates are given multiplied by $2\pi r$, where r is the radius, to eliminate the effect due to the cylindrical geometry. The statistical errors are given for the 68.3% confidence level. The solid line shows the calculated gamma-ray heating rates in stainless steel. The C/E values are shown in Figure 13. The error bars in this figure represents the statistical errors only. The vertical dashed lines show the FBBF outer transformer/inner blanket interface at R = 0.22m, the inner blanket/outer blanket interface at R = 0.57m, and the outer blanket/reflector interface at R = 0.74m.

The measured gamma-ray heating rates in lead for radial traverses is shonw in Figure 14. The solid lines show the calculated gamma-ray heating rates in lead. The C/E values are shown in Figure 15.

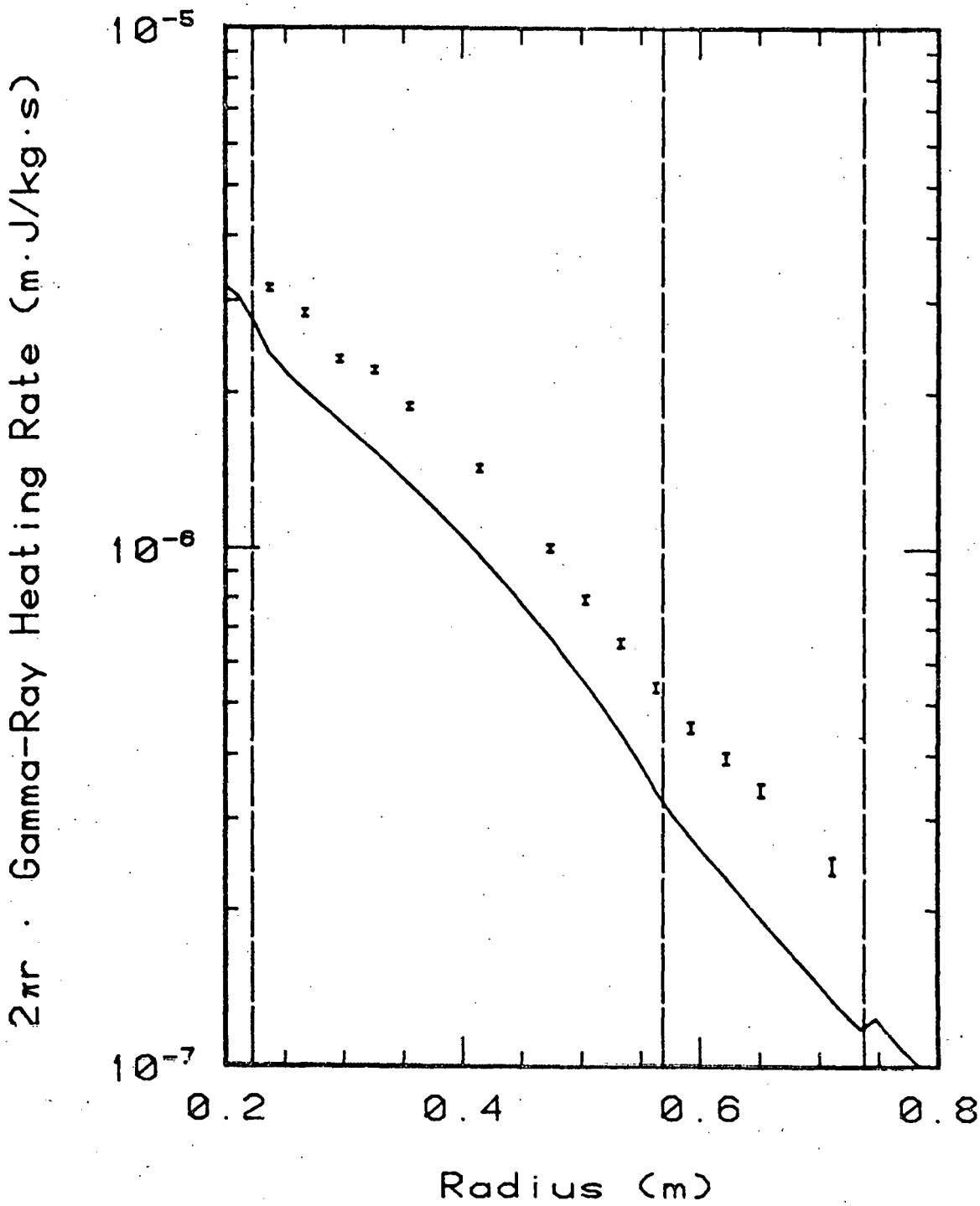

Figure 12:
Measured gamma-ray heating rates in stainless steel for a radial traverse at the transformer axial midplane. The error bars represent the statistical errors only. The solid line shows the calculated gamma-ray heating rates in stainless steel. The vertical dashed lines show the FBBF blanket interfaces.

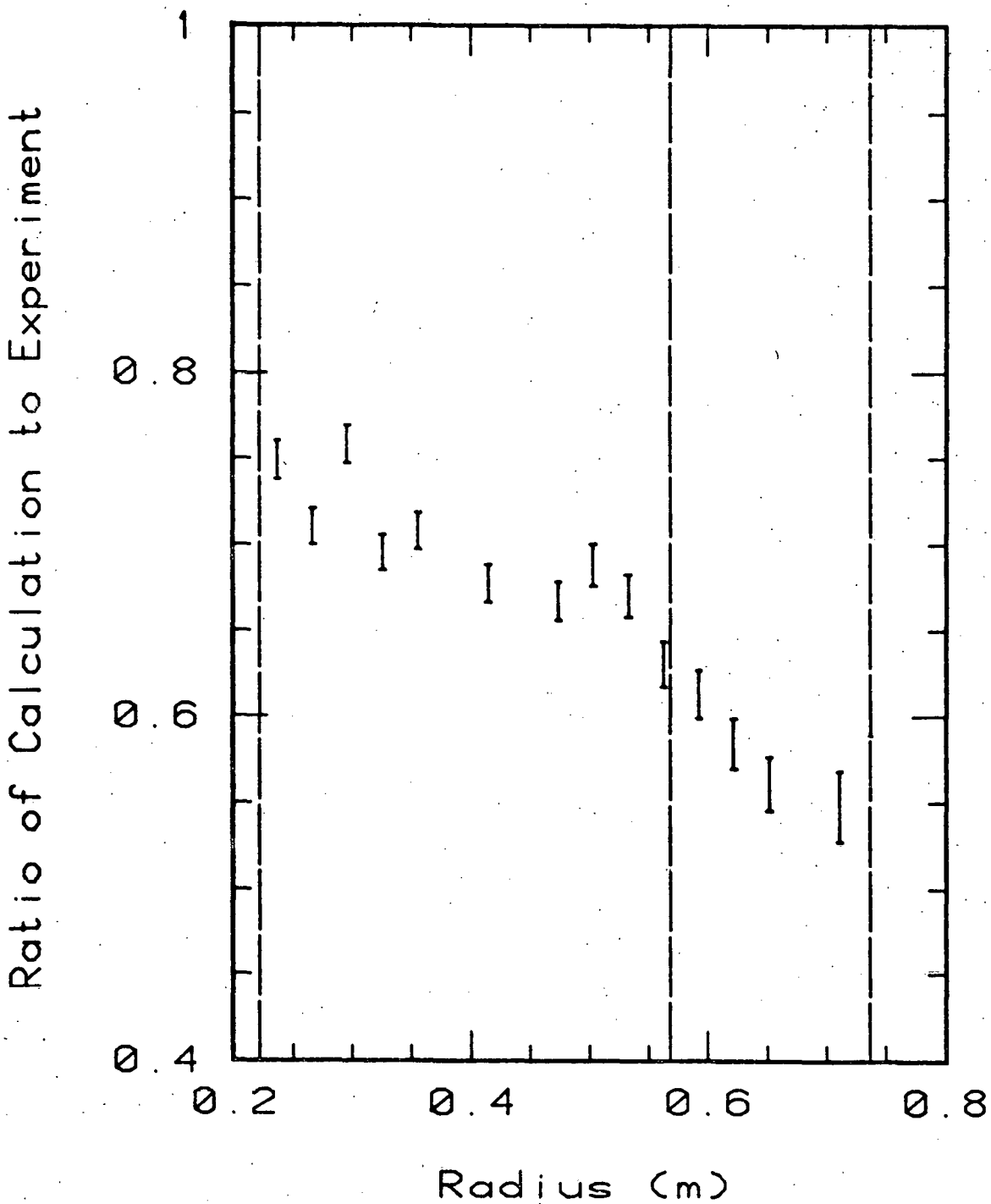

Figure 13:
Ratio of calculated to measured gamma-ray heating rates in stainless steel for a radial traverse at the transformer axial midplane. The error bars represent the statistical errors only. The vertical dashed lines show the FBBF blanket interfaces.

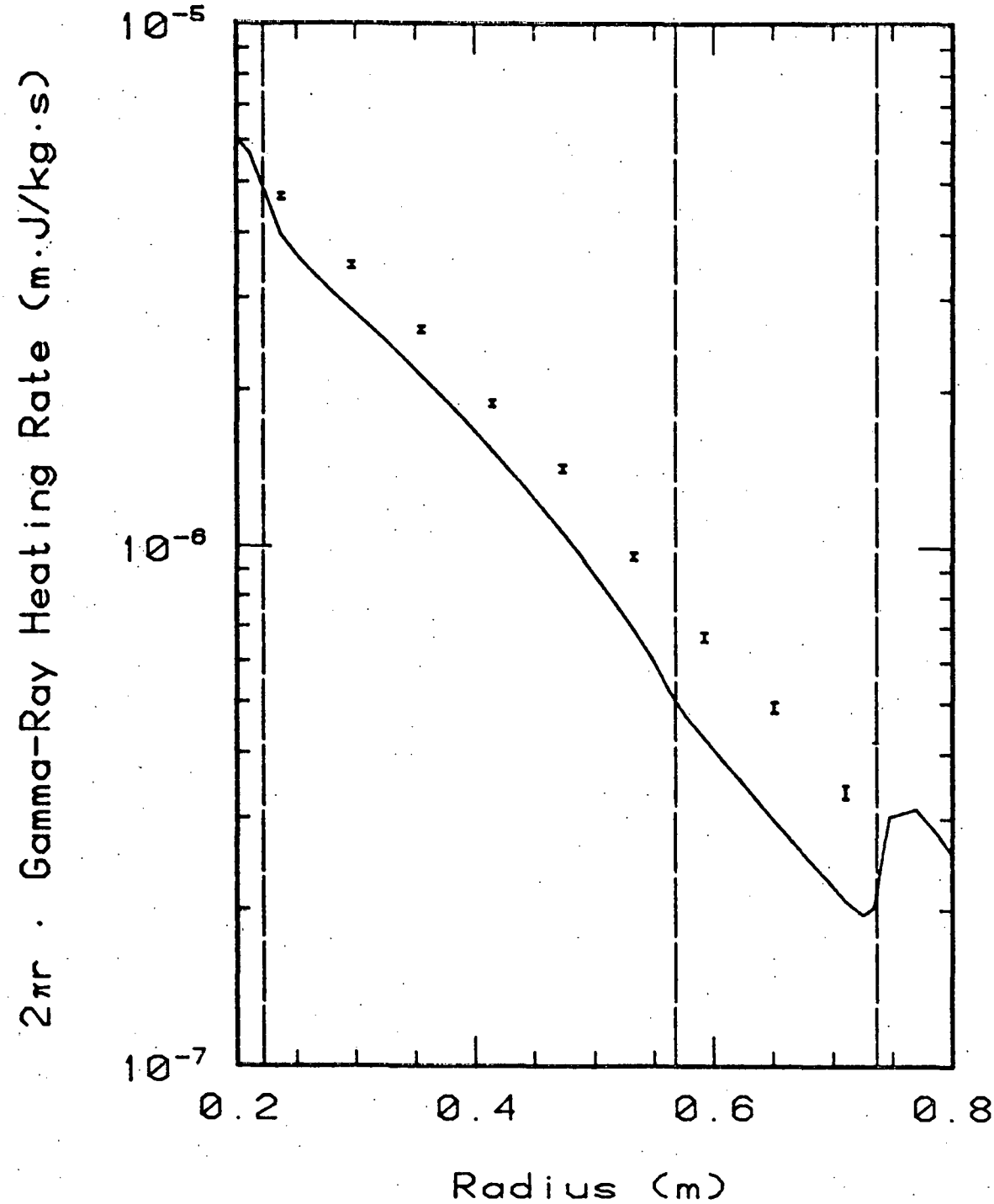

Figure 14:
Measured gamma-ray heating rates in lead for a radial traverse at the transformer axial midplane. The error bars represent the statistical errors only. The solid line shows the calculated gamma-ray heating rates. The vertical dashed lines show the FBBF blanket interfaces.

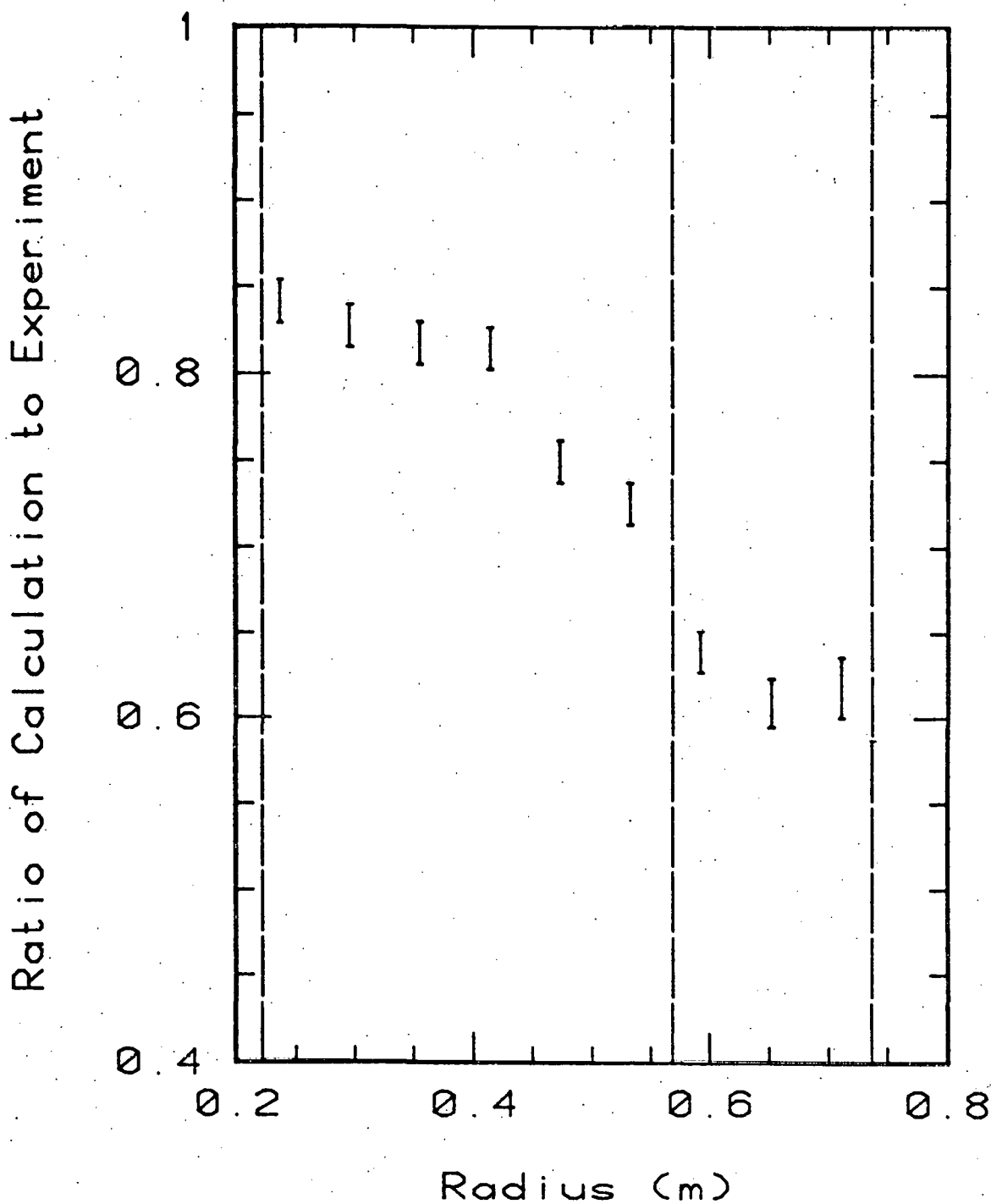

Figure 15:
Ratio of calculated to measured gamma-ray heating rates in lead for a radial traverse at the transformer axial midplane. The error bars represent the statistical errors only. The vertical dashed lines show the FBBF blanket interfaces.

From the stainless steel and lead radial traverse results it is seen that the calculation underestimates the measured gamma-ray heating raes in the FBBF blanket. This underestimation is seen in both stainless steel and lead. The underestimation by the calculation of the gamma-ray heating in stainless steel is approximately 25% at the inside of the blanket. This underestimation becomes increasingly larger for increasing blanket radii. At the outside of the blanket, the calculation underestimates the stainless steel gamma-ray heating rate by roughly 45% to 50%. This underestimation of the stainless steel gamma-ray heating rates is easily seen in Figures 12 and 13. The same trend is seen for gamma-ray heating in lead (see Figures 14 and 15). However, the underestimation at the inside of the blanket is approximately 10% in lead as compared to the 25% seen in stainless steel. The underestimation at the outside of the blanket is 40% in lead.

An almost identical trend of the calculation underestimating the experiment is seen in the radial traverse measurements of the ^{239}U capture rate.[7] In the gamma-ray flux calculation it was seen that the ^{238}U capture reaction dominated the production of gamma rays in the FBBF blanket. Thus, the underestimation of the ^{238}U capture rates by the neutron flux calculation causes a correpsonding underestimation of the gamma-ray heating rates by the gamma-ray flux calculation. Much of the discrepancy between the calculated and measured gamma-ray heating rates can thus be explained by the underestimation of the ^{238}U capture rates by the neutron flux calculation.

Another conclusion can be made from the fact that the C/E values for the gamma-ray heating rates are similar to the C/E values for the

^{238}U capture rates. Since the ^{238}U capture reaction dominates the production of gamma rays, the spatial distribution of the gamma-ray source follows the spatial distribution of the ^{238}U capture reaction. Then, since the C/E values of the ^{238}U capture rates and the gamma-ray heating rates exhibit the same trends, it can be concluded that in the FBBF the source distribution of the gamma rays is more important than the transport. If the transport of gamma rays was important, one would expect to see a gamma-ray heating rate distribution that is different from the ^{238}U capture rate distribution.

The comparison of the stainless steel C/Es with the lead C/Es shows that the gamma-ray heating rates in stainless steel are underestimated by the calculation by roughly 14% more than the heating rates in lead. This problem is attributed to an underestimation of the calculated gamma-ray heating rates in stainless steel.

II.D Neutron Capture Rate Measurements

(G. Harms and F. Clikeman)

Measurements of the neutron capture rates for ^{238}U, ^{232}Th, ^{197}Au, ^{186}W, ^{98}Mo, ^{23}Na, ^{55}Mn, ^{60}Co, ^{181}Ta, ^{45}Sc, ^{109}Ag, and ^{58}Ni have been completed in blanket I. In addition, the reactions $^{115}In(n,n')$ and $^{58}Ni(n,p)$ have also been investigated. The absolute activities for each of these reactions has been determined using gamma-ray spectroscopy. The same reaction are being measured in blankets IIA and IIB and the results together with a detailed discusion of the methods used will be presented in a seperate project report. Some preliminary results are presented in Sec. III together with a discussion of the calculational methods that are being investigated.

III. COMPUTER CALCULATIONS AND METHOD DEVELOPMENT

(G. Harms and F. Clikeman)

Calculations of the neutron reaction rates in the FBBF facility have been performed using the two-dimensional diffusion code 2DB[4]. Region-dependent cross sections for the calculations are generated using the one-dimensional diffusion code 1DX[9]. Resonance self shielding is treated in 1DX by the Bondarenko self-shielding factor method[6]. The 50-group library LIB-IV[8], which includes the information necessary to perform temperature and composition dependant resonance self shielding, was used as the data base for the group constant generation. Originally, the 1DX calculations required to collapse the 50 group LIB-IV group constants to the 30-group set used in 2DB for the FBBF calculations were performed at Argonne National Laboratory. During the past year, a version of 1DX has been made operational on the Purdue University computers. This permits a greater number of calculational methods to be investigated as well as sensitivity studies of various cross sections in order to determine which factors have the greatest influence on agreement with the experiments.

For the present work, a 50-group set of self-shielded cross sections has been obtained for the seven material regions that intersect the midplane of the FBBF. A one-dimensional model of the facility has also been developed and used with the cross sections in a 50-group flux calculation. The results of this calculation were used to collapse the 50-group cross sections to a 30-group set. The same calculation was used to generate the 30-group cross sections for the off-midplane

material regions. The cross section calculations were made with the code 1DX. The 30-group cross sections were then used in a two-dimensional (r - z) diffusion calculation to obtain the neutron fluxes in the FBBF.

In the shielding factor approach to resonance self shielding, the neutron flux $\phi(E)$ in the neighborhood of a resonance is assumed to be of the form

$$\phi(E) = \frac{C(E)}{\sigma_o + \sigma_t(E)}$$

where

$C(E)$ = slowly varying component of the flux,

$\sigma_t(E)$ = microscopic total cross section of the species being self shielded, and

σ_o = cross sections of all of the other species present in the material per nucleus of the species being self shielded.

This flux can be used to generate group cross sections σ_g by

$$\sigma_g = \frac{\int_g \sigma(E)\ \phi(E)\ dE}{\int_g \phi(E)\ dE}$$

where $\sigma(E)$ is the microscopic cross section being collapsed and the integrals are taken over the energy limits of the group. The composition dependence of the self shielding calculation enters by way of the σ_o, called the background cross section. A resonance in $\sigma(E)$ will be

accompanied by a resonance in $\sigma_t(E)$ and thus by a depression in $\phi(E)$. The depth of the depression will be determined by the change in $\sigma_t(E)$ relative to σ_o. The depression in the flux at the resonance energy of $\sigma(E)$ results in a reduction of the group cross section σ_g. For a given resonance, it is evident that large values of σ_o give small self shielding corrections while the reverse is true for small background cross sections.

In the first set of reaction rate calculations, the FBBF was treated as a series of homogeneous regions. The total number of nuclei for each nuclear species in a region was calculated and divided by the region volume to obtain the homogenized number density for that species. Each region was then assumed to contain a single material with the calculated number density of each species. For regions that are assumed to be homogeneous, each element (i.e. iron, uranium, oxygen, etc.) in each material (i.e. stainless steel, uranium dioxide, etc.) in a given region (i.e. blanket, reflector, ect.) contributes to the background cross section for every other element. In reality, the FBBF is a heterogeneous combination of fuel, cladding, voids, structure, etc.

For neutrons that have a long mean free path in the local material, the homogeneous treatment of the regions is adequate. However, neutrons at the energy of a strong resonance of a given element have a short mean free path in materials containing that element and a long mean free path in materials void of that element. For example, neutrons at the energy of an iron resonance will have a short mean free path in the stainless steel cladding and a long mean free path in the aluminum cladding and the UO_2 fuel. Thus, neutrons at this energy will be primarily affected

while traversing the stainless steel cladding and will be relatively unaffected while in the aluminum cladding and the UO_2 fuel. Since cross section self shielding is an attempt to account for the behavior of neutrons at resonance energies, the distances that must be considered are of the order of the mean free path of resonance energy neutrons. For a neutron in a 5000 barn ^{238}U resonance in the blanket fuel, this distance is about 0.1 mm. Thus, the FBBF appears to be heterogeneous assembly to neutrons at resonance energies.

To account for this apparent hetergeneity for resonance effects, a new set of group constants was generated in which each blanket material was treated separately. For this preliminary calculation, the 50-group fluxes obtained in the one-dimensional calculation were used to collapse cross sections for three new materials. The three new materials had the elements and number densities of the stainless steel, aluminum, and UO_2 fuel for the first loading of the FBBF blanket and were self shielded separately. The effect of this revised procedure was to increase the resonance self shielding for each element by decreasing the number of materials that contribute to the background cross section. A new set of homogeneous blanket group constants was obtained by mixing the newly collapsed cross sections into region materials with the original homogeneous number densities. The only change to this set was in the blanket material self shielding. The new set of group constants with the modified blanket cross section was used as input to 2DB and the flux recalculated. For this calculation, the FBBF regions were once again treated as homogeneous materials.

Figures 16 through 19 give a comparison between the normalized neutron flux spectra of the calculations with the blanket materials self shielded homogeneously and the calculations with the blanket materials self shielded separately. The comparisons are made for spectra calculated at four different radii. The most notable change between the two spectra at each location is in the magnitude of the depression apparent in group 12 (24.8 keV to 40.1 keV). This depression is the combined effect of a 28 keV iron resonance and a 33 keV aluminum resonance. The differences between the two spectra in Fig. 19 for group 12 are washed out because the spectra at 0.711 m are strongly influenced by neutrons returning from the reflectors where the cross sections were the same for both calculations.

The ratio of the calculated to experimental (C/E) capture rates for ^{238}U and ^{197}Au are shown in Figs. 20 and 21 for the calculations with the blanket materials self-shielded homogeneously. The error bars in these and the following figures indicate only the statistical uncertainty in the capture rate measurements. Both the calculations and the measurements were made on an absolute basis for a source strength of 10^{10} neutrons per second. Thus no normalization between the calculations and measurements is required. The C/E values for both reactions show significant downward trends across the inner blanket (through about 0.55 m).

The C/E values for the gold reaction turn around and increase across the outer blanket (0.55 to 0.71 m) but continue the downward trend for ^{238}U capture.

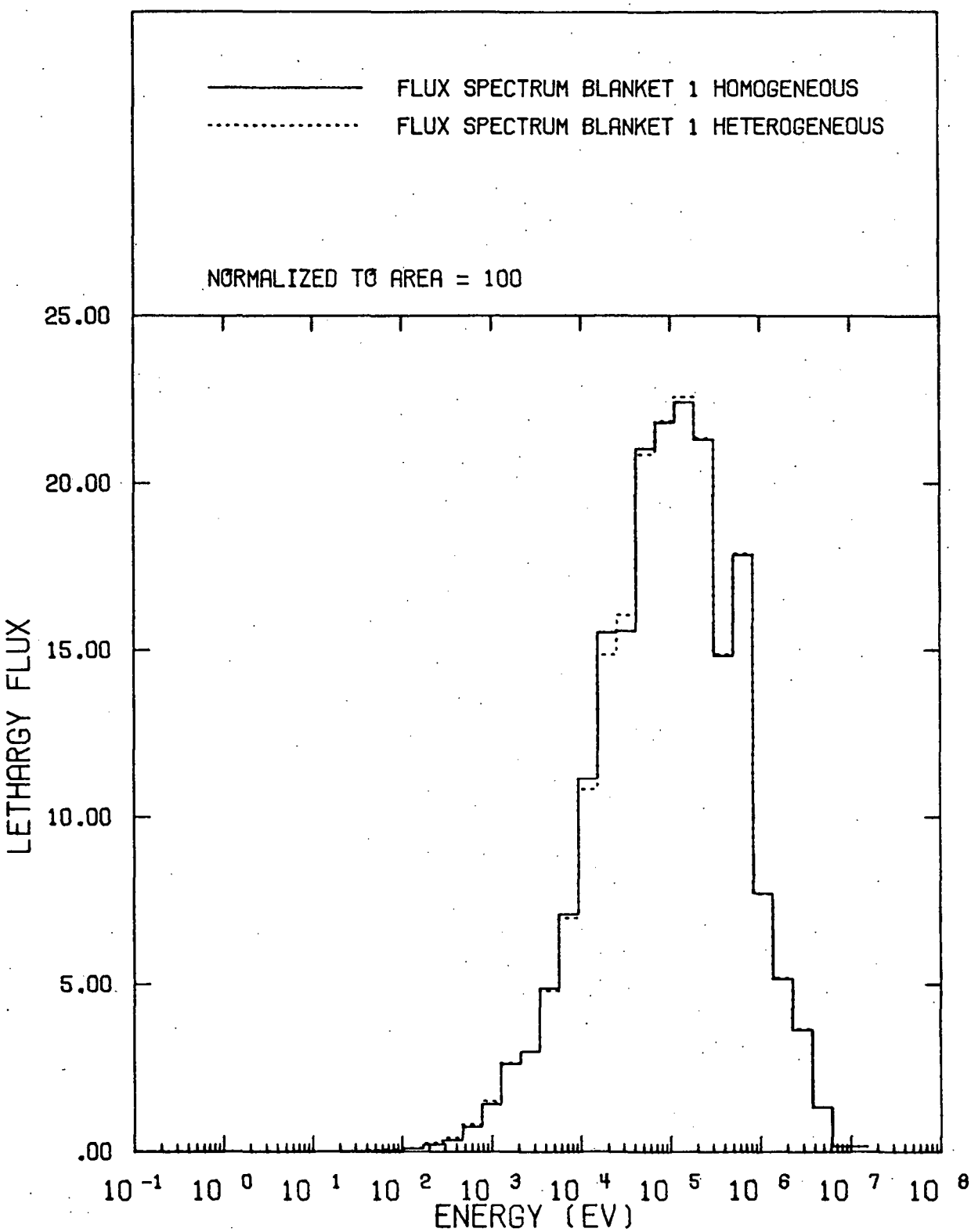

Figure 16:
Comparison of the neutron spectra calculated for the cases of homogeneous blanket self shielding (solid line) and heterogeneous blanket self shielding (dashed line) at a radius of 0.236 m.

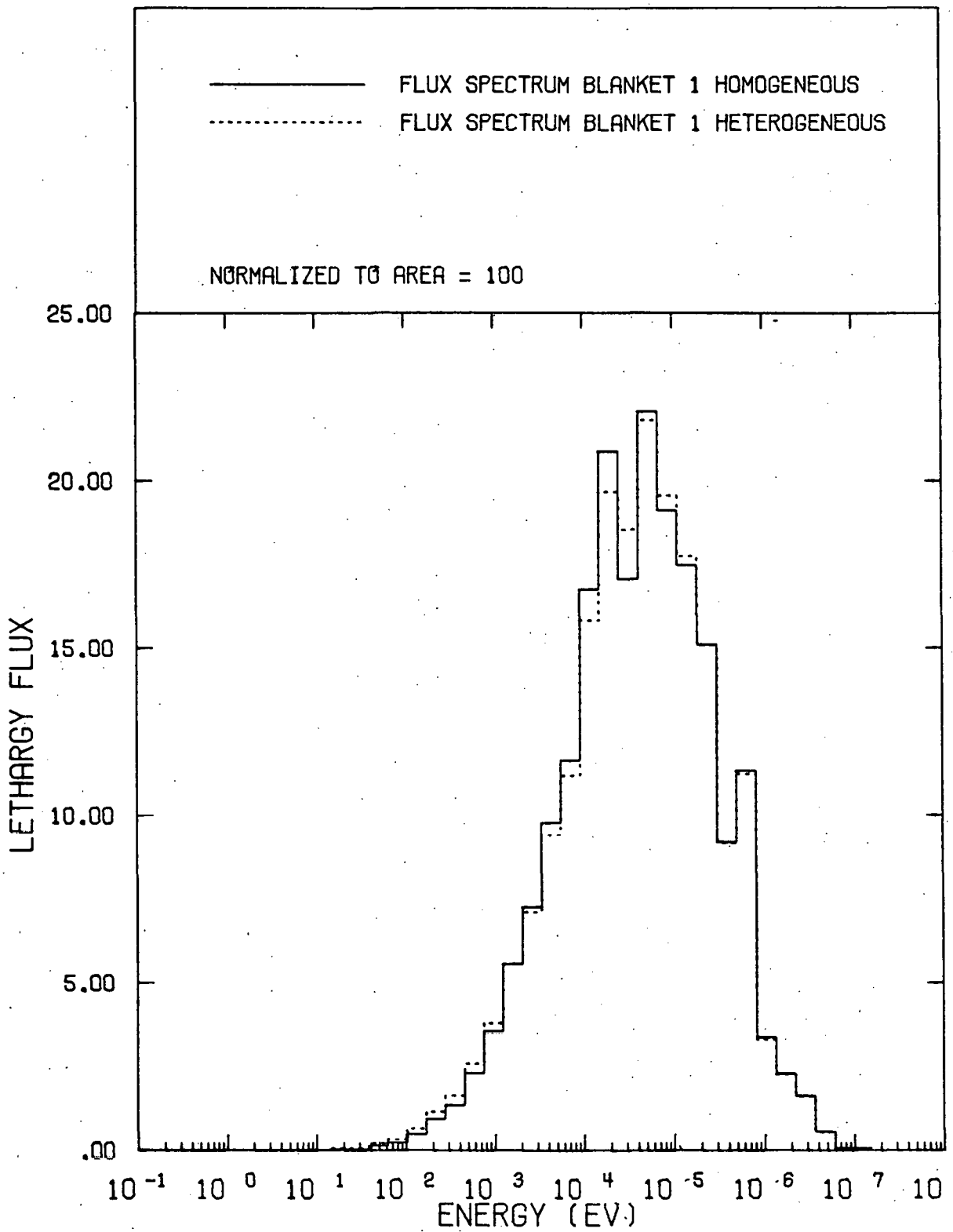

Figure 17:
Comparison of the neutron spectra calculated for the cases of homogeneous blanket self shielding (solid line) and heterogeneous blanket self shielding (dashed line) at a radius of 0.385 m.

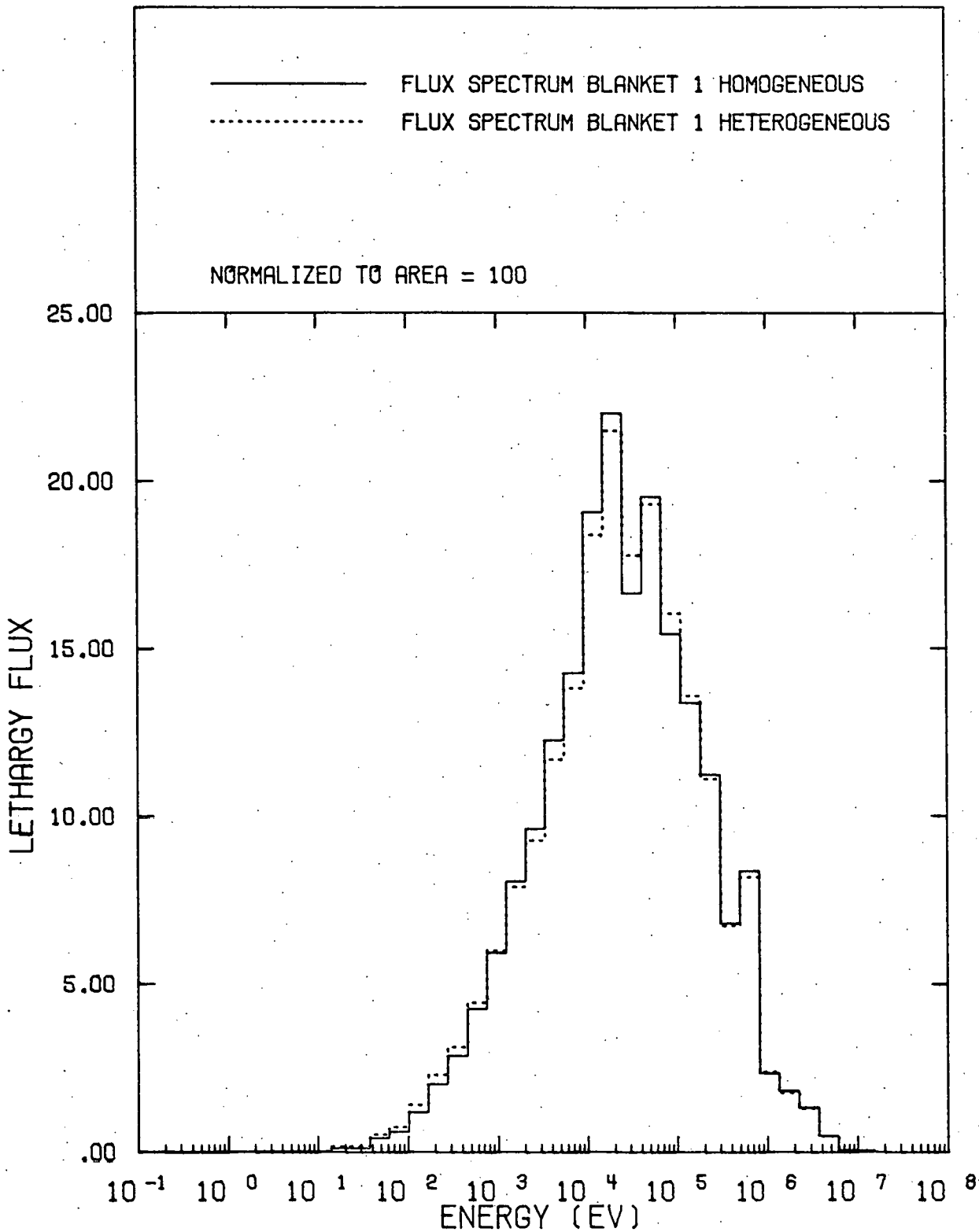

Figure 18:
Comparison of the neutron spectra calculated for the cases of homogeneous blanket self shielding (solid line) and heterogeneous blanket self shielding (dashed line) at a radius of 0.563 m.

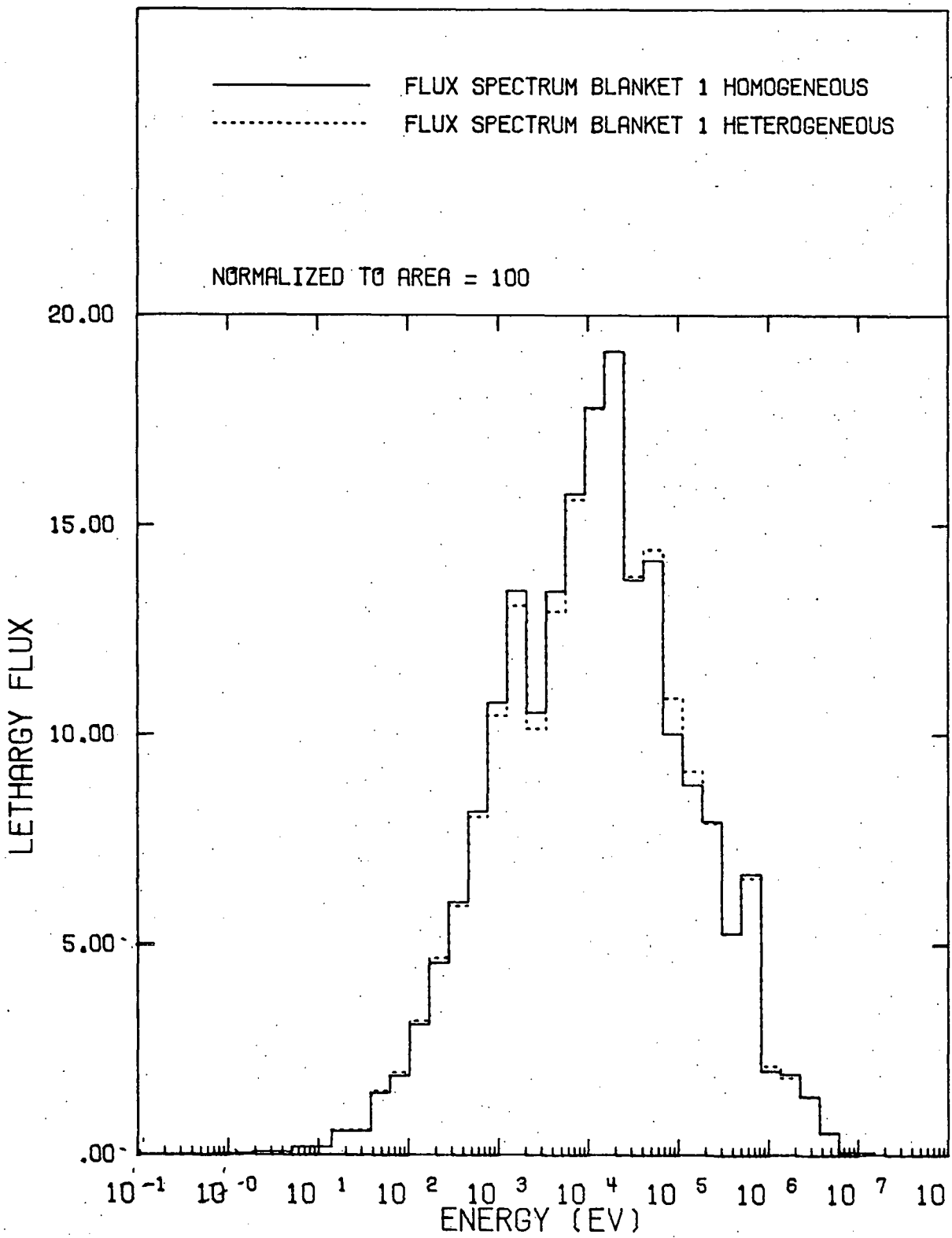

Figure 19
Comparison of the neutron spectra calculated for the cases of homogeneous blanket self shielding (solid line) and heterogeneous blanket self shielding (dashed line) at a radius of 0.711 m.

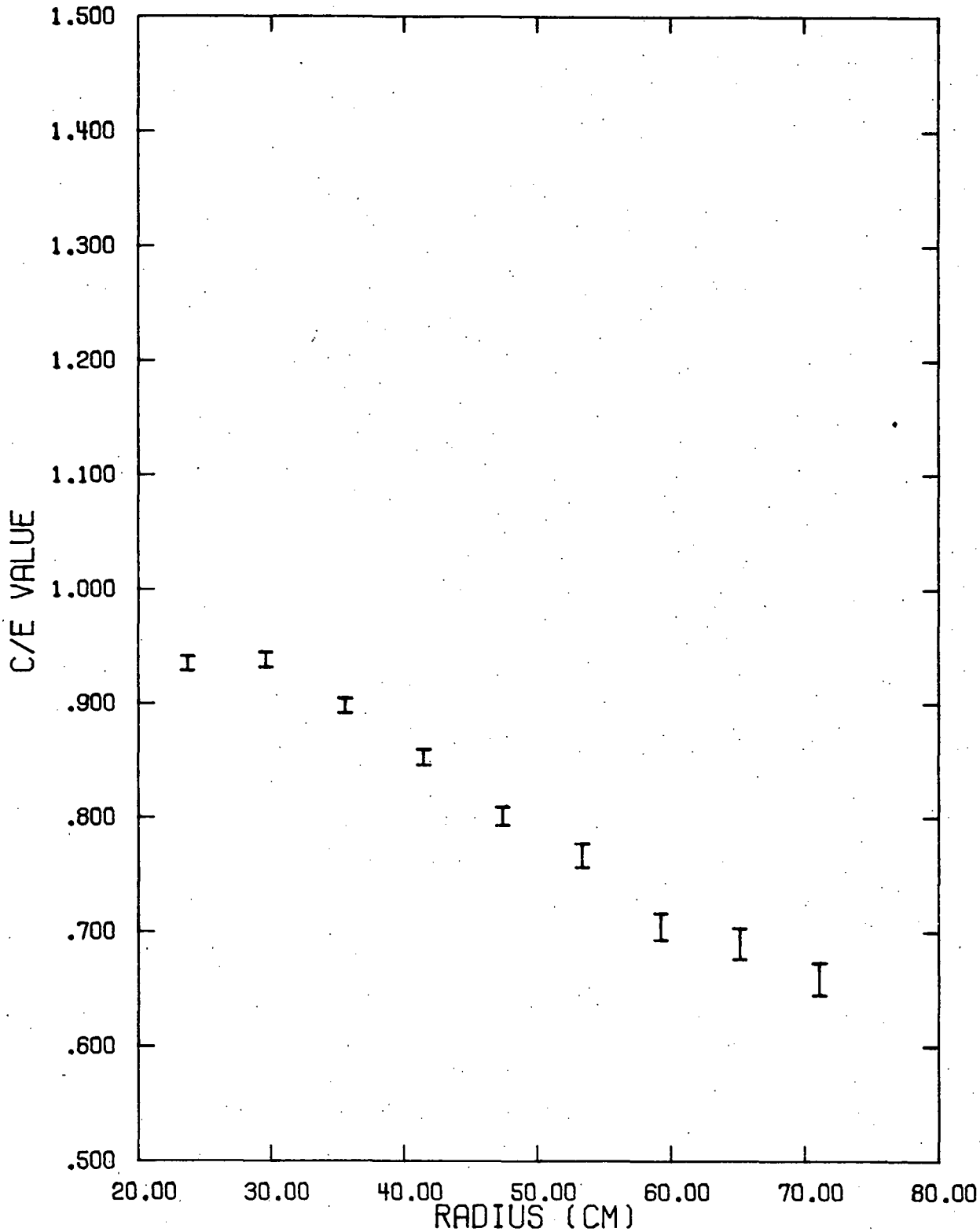

Figure 20:
Ratio of calculated to experimental ^{238}U capture rates for the calculations with homogeneously self-shielded blanket materials

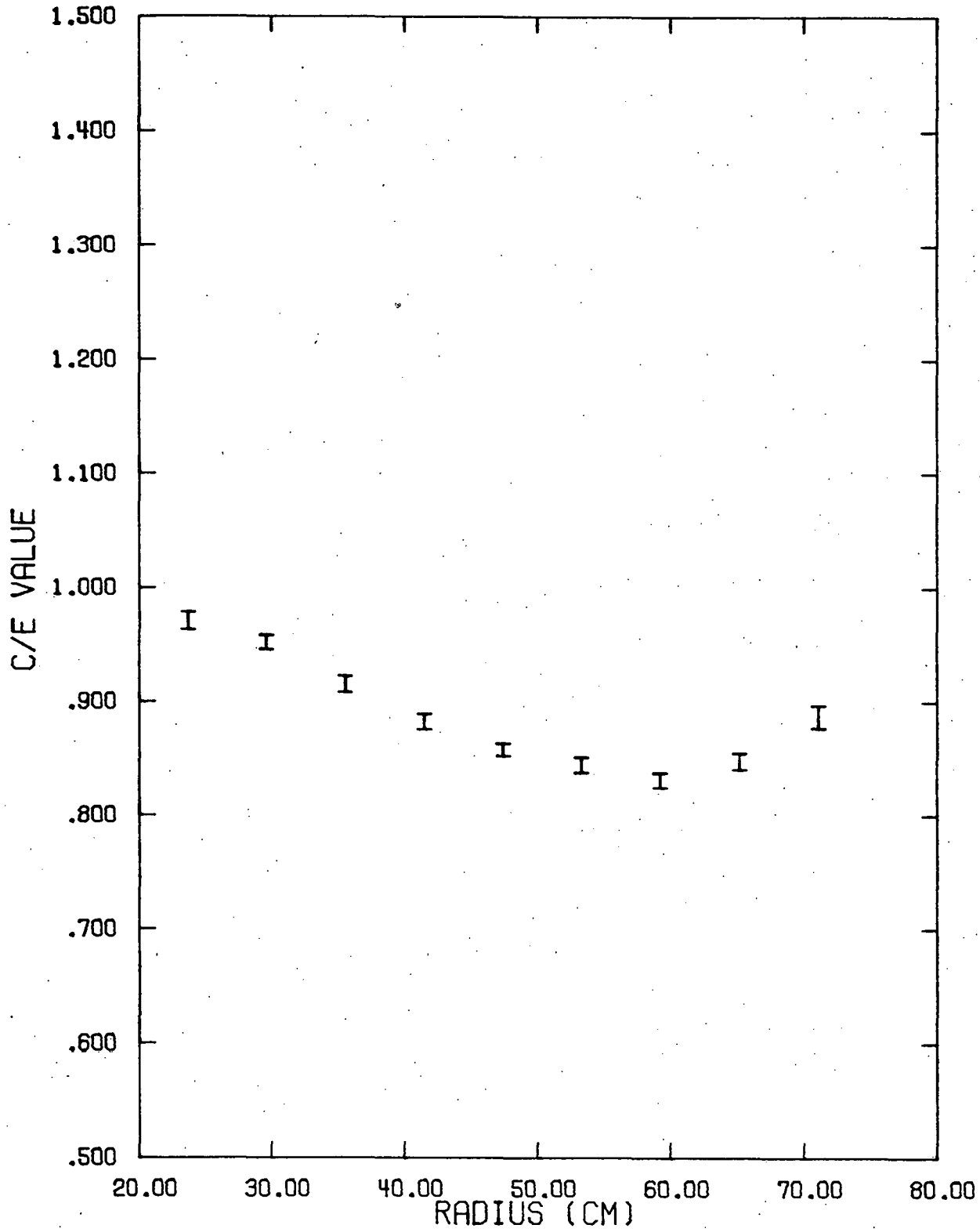

Figure 21
Ratio of calculated to experimental ^{197}Au capture rates for the calculations with homogeneously self-shielded blanket materials

The C/E ratios for the calculation involving the heterogeneous self-shielding treatment are shown in Figs. 22 and 23 for ^{238}U and ^{197}Au capture resectively. The C/E values for ^{238}U again show a downward trend but do not drop off as steeply as in Fig. 20. The C/E values for ^{197}Au capture are distributed around unity and show no easily discernable trend. Ideally, the perfect calculation and the perfect measurement should give constant C/E values of 1. Based only on the ^{238}U and ^{197}Au capture rates, the change from homogeneous to heterogeneous self shielding appears to be a significant step in the right direction and warrants further investigation.

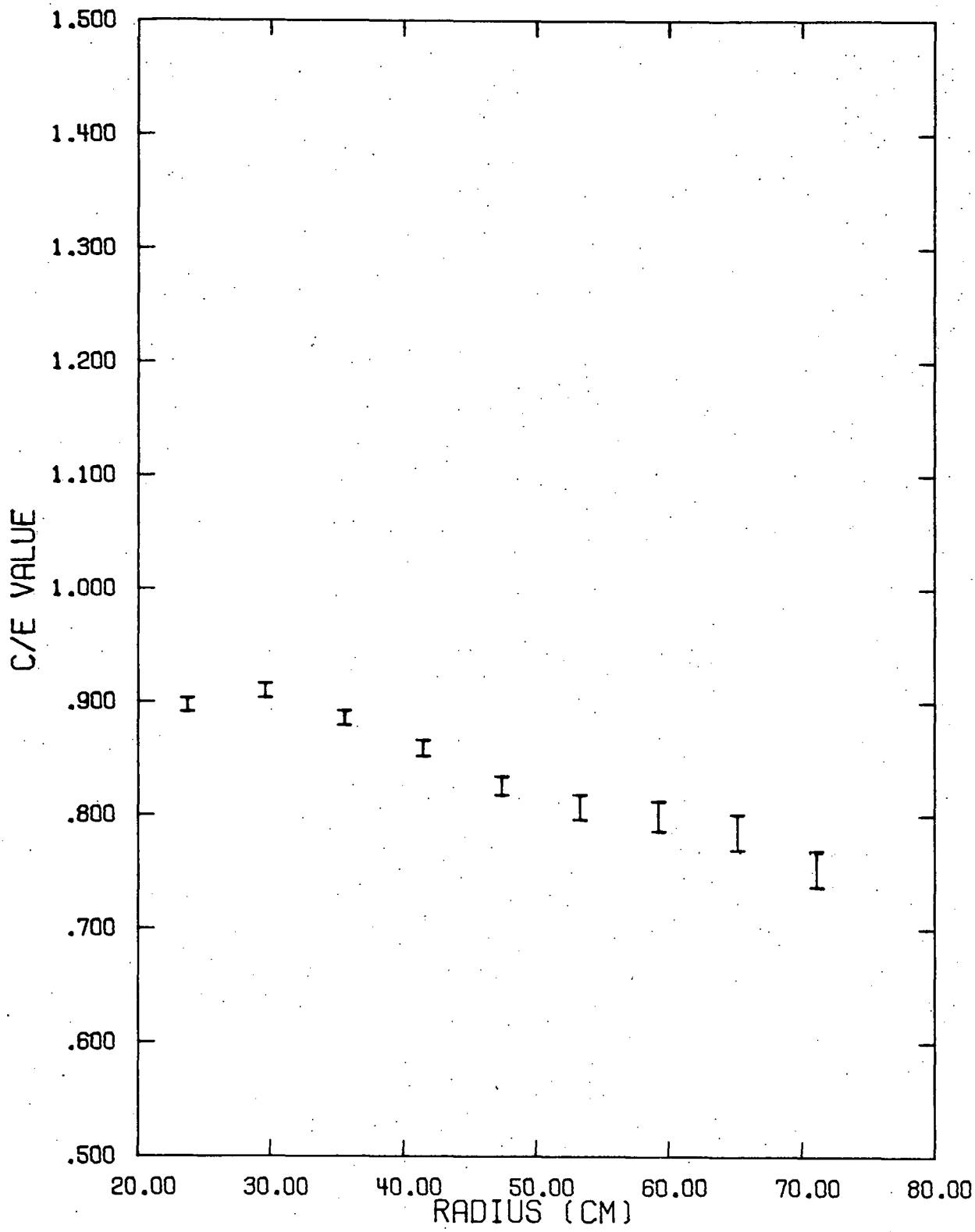

Figure 22:
Ratio of calculated to experimental ^{238}U capture rates for the calculations with heterogeneously self-shielded blanket materials

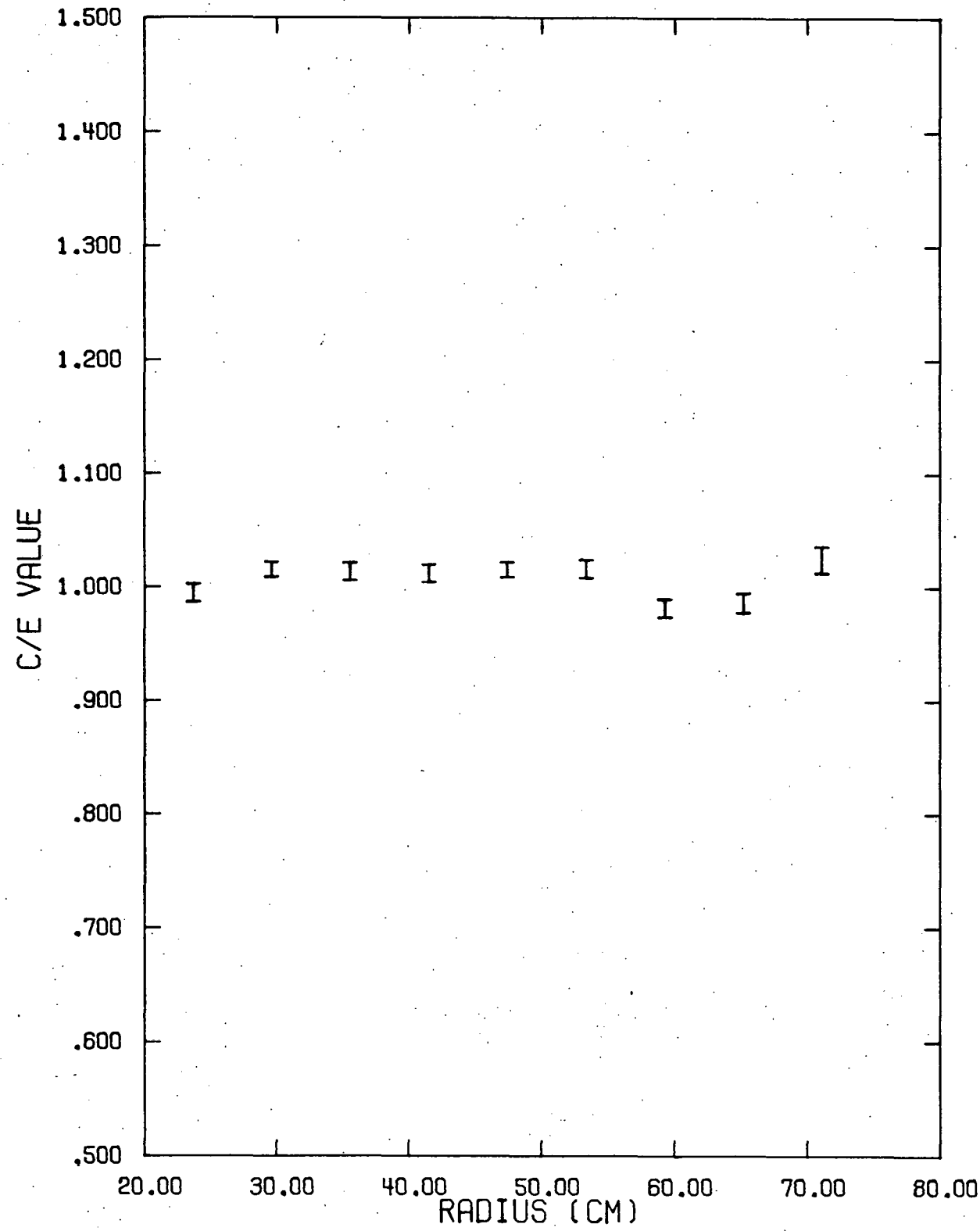

Figure 23:
Ratio of calculated to experimental ^{197}Au capture rates for the calculations with heterogeneously self-shielded blanket materials

IV. CONCLUSIONS

The conclusions that can be drawn from the research that has been completed to date on the FBBF project support the original contentions that diffusion theory may not work well in the external blanket regions of fast reactors. Results from the fission rate measurements show that the calculations using homogeneous regions for the blanket underpredict the measured ^{235}U and ^{239}Pu fission rates by 25% in the outer regions of the blanket. The measurements of the ^{238}U capture rate show the same results. On the other hand, threshold fission reactions in ^{238}U agree well with the calculations, but ^{237}Np and ^{232}Th threshold fission rates exhibit trends similar to the other fission rates.

Spectrum measurements show that the calculated spectra tend to be softer than the measurements indicate. This would probably be true if the calculated fission rates were underpredicted; a result supported by the fission rate measurements. Alternately, overestimating the scattering, especially inelastic scattering, would also result in a softer calculated spectrum. Present fission rate and spectrum measurements can not resolve the reasons why the ^{238}U fission rates do not show the same trend as the other reaction rates.

Thermoluminescent dosimeter measurements of the gamma-ray heating also show that the calculations underpredict the experiment. In fact, the trend in the C/E values of the gamma-ray heating follow closely the C/E values of the ^{238}U capture. This is to be expected since the neutron capture in ^{238}U is predicted to be the largest source of gamma rays. The trends in the measurements show that the distribution of the

gamma-ray sources rather than the transport of the gamma rays dominate the gamma-ray heating distributions in the FBBF. More work, however, is required to improve the agreement in the magnitudes of the calculated gamma-ray heating rates and/or in the corrections used to determine the gamma-ray heating rates from the TLD measurements.

Problems with the existing calculations of the neutron spectra and reaction rate in the FBBF can come from three sources; the applicability of diffusion theory, cross sections, and heterogeneity effects. Although some of the basic assumptions of diffusion theory, such as the separability of the space and energy dependence of the neutron flux do not hold in the blanket regions, it is still convenient to use diffusion theory for blanket calculations. Although agreement between calculations and experiment is better when Monte Carlo transport calculations are made, the agreement still is not good.

The problem in nuclear cross sections can arise from the use of aluminum in the blankets. Work in progress on blanket II should determine if the aluminum cross sections are contributing significantly to the disagreement between theory and experiment.

The first attempts at modifying the self shielding of the resources to compensate for the heterogeneity of the blanket look promising and indicate that the heterogeneity effects may be a major contribution to the disagreement between theory and experiment. Inproved calculations and extending the treatment to more materials should verify if this is indeed the source of disagreement and a solution to the problem.

REFERENCES

1. H. P. Chou, "Absolute Fission Rate Measurements in the Fast Breeder Blanket Facility," Ph.D. Thesis, School of Nuclear Engineering, Purdue University (1981).

2. D. W. Vehar, "Measurements of Neutron Energy Spectra in the Fast Breeder Blanket Facility," Ph.D. Thesis, School of Nuclear Engineering, Purdue University (1980).

3. H. P. Chou, R. H. Johnson, and F. M. Clikeman, "An Automatic Fission Track Scanner," Nucl. Inst. and Meth. 185, 359 (1981).

4. W. W. Little, Jr. and R. W. Hardie, "2DB User's Manual-- Revision 1," BNWL-821-REV1 (1969).

5. E. M. Gelbard and R. E. Prael, "Monte Carlo Work at Argonne National Laboratory," Proc. NEACRP Meeting of a Monte Carlo Study Group, Argonne National Laboratory, 1-3 July 1974, ANL-75-2, NEA-CRP-L-118 (1975).

6. I. I. Bondarenko, ed., Group Constants for Nuclear Reactor Calculations, Consultants Bureau (1964).

7. R. H. Johnson, F. M. Clikeman, H. P. Chou, and G. A. Harms, "Fission Rates and ^{238}U Capture Rates for Loading 1 of the Fast Breeder Blanket Facility," COO-2826-15, PNE-81-150, School of Nuclear Engineering, Purdue University (June 1981).

8. R. B. Kidman and R. E. McFarlane, "LIB-IV, A Library of Group Constants for Nuclear Reactor Calculations," LA-6287-MS (1976).

9. R. W. Hardie and W. W. Little, Jr., "1DX, A One- Dimensional Diffusion Code for Generating Effective Nuclear Cross Sections," BNWL-460 (1968).

10. "ANISN-W, A Multigroup One-Dimensional Discrete Ordinates Transport Code with Anisotropic Scattering," Radiation Shielding Information Center, Oak Ridge National Laboratory, Oak Ridge, Tennessee, CCC-255.

11. "DLC-37/EPR, Coupled 100-Group Neutron 21-Group Gamma-Ray Cross Sections for EPR Neutronics," Radiation Shielding Information Center, Oak Ridge National Laboratory, Oak Ridge, Tennessee, DLC-37/EPR.